

1  
2  
3  
4  
5  
6  
7  
8  
9  
10  
11  
12  
13  
14  
15  
16  
17  
18  
19  
20  
21  
22  
23  
24  
25  
26  
27  
28  
29  
30  
31  
32  
33  
34  
35  
36

## **Coastal Sea Level rise at Senetosa (Corsica) during the Jason altimetry missions**

Yvan Gouzenes<sup>1</sup>, Fabien Léger<sup>1</sup>, Anny Cazenave<sup>1,2</sup>, Florence Birol<sup>1</sup>, Pascal Bonnefond<sup>3</sup>,  
Marcello Passaro<sup>4</sup>, Fernando Nino<sup>1</sup>, Rafael Almar<sup>1</sup>, Olivier Laurain<sup>5</sup>, Christian Schwatke<sup>4</sup>,  
Jean-François Legeais<sup>6</sup> and Jérôme Benveniste<sup>7</sup>

1.LEGOS, Toulouse; 2. ISSI, Bern; 3. Observatoire de Paris-SYRTE, Paris ; 4. TUM,  
Munich; 5. Observatoire de la Côte d'Azur-Géoazur, Sophia-Antipolis; 6. CLS, Ramonville  
St Agne; 7. ESA-ESRIN, Frascati.

**3<sup>rd</sup> Revision**

**9 August 2020**

Corresponding author: Anny Cazenave ([anny.cazenave@legos.obs-mip.fr](mailto:anny.cazenave@legos.obs-mip.fr); [anny.cazenave@gmail.com](mailto:anny.cazenave@gmail.com))

37  
3839 **Abstract**

40 In the context of the ESA Climate Change Initiative project, we are engaged in a regional  
41 reprocessing of high-resolution (20 Hz) altimetry data of the classical missions in a number of  
42 world's coastal zones. It is done using the ALES (Adaptive Leading Edge Subwaveform)  
43 retracker combined with the X-TRACK system dedicated to improve geophysical corrections  
44 at the coast. Using the Jason-1&2 satellite data, high-resolution, along-track sea level time  
45 series have been generated and coastal sea level trends have been computed over a 14-year  
46 time span (from July 2002 to June 2016). In this paper, we focus on a particular coastal site  
47 where the Jason track crosses land, Senetosa, located south of Corsica in the Mediterranean  
48 Sea, for two reasons: (1) the rate of sea level rise estimated in this project increases significantly  
49 in the last 4-5 km to the coast, compared to what is observed further offshore, and (2)  
50 Senetosa is the calibration site for the Topex/Poseidon and Jason altimetry missions,  
51 equipped for that purpose with in situ instrumentation, in particular tide gauges and GNSS  
52 antennas. A careful examination of all the potential errors that could explain the increased  
53 rate of sea level rise close to the coast (e.g., spurious trends in the geophysical corrections,  
54 imperfect intermission bias estimate, decrease of valid data close to the coast and errors in  
55 waveform retracking) has been carried out, but none of these effects appear able to explain  
56 the trend increase. We further explored the possibility it results from real physical processes.  
57 Change in wave conditions was investigated but wave set up was excluded as a potential  
58 contributor because of too small magnitude and too localized in the immediate vicinity of  
59 the shoreline. Preliminary model-based investigation about the contribution of coastal currents  
60 indicates that it could be a plausible explanation of the observed change in sea level trend  
61 close to the coast.

62

## 63 **1. Introduction**

64 Since the early 1990s, satellite altimetry provides invaluable observations of the global mean  
65 sea level and its regional variability. In the recent years, this data set has generated an  
66 abundant literature on the processes causing sea level change at global and regional scales, as  
67 well as on closure of the sea level budget (e.g., Church et al., 2013, Stammer et al., 2013,  
68 Dieng et al., 2017, Nerem et al., 2018, WCRP, 2018, SROCC, 2019). In addition to the global  
69 mean rise and superimposed regional trends, changes in small scale processes such as local  
70 atmospheric effects, baroclinic instabilities, coastal trapped waves, shelf currents, waves,  
71 fresh water input from rivers in estuaries, can substantially modify the rate of sea level change  
72 at the coast compared to open sea regions (Woodworth et al., 2019, Melet et al., 2018,  
73 Piecuch et al., 2018, Dodet et al., 2019, Durand et al., 2019). In addition, ground subsidence  
74 may amplify the rate of sea level change at the coast (Woppelmann and Marcos, 2016). In  
75 terms of societal impacts, what really matters in the coastal zone is indeed the sum of the  
76 global mean sea level rise plus the regional trends and the local processes.

77 Up to recently, due to land contamination of radar echoes and less precise geophysical  
78 corrections, classical altimetry did not provide reliable sea level data in a band of 10-15 km  
79 along coastlines. However different studies have shown that using adapted reprocessing of  
80 altimetry measurements and improving geophysical corrections allows retrieving a large  
81 amount of valid sea level close to the coast (e.g., Cipollini et al., 2018, Passaro et al., 2015,  
82 Marti et al., 2019). In addition, despite having a much higher noise level than the classical 1  
83 Hz altimetry data, high-resolution 20 Hz measurements allow to recover more information on  
84 coastal sea level variations (Birol and Delebecque, 2014, Leger et al., 2019).

85 In the context of the Climate Change Initiative (CCI) project of the European Space  
86 Agency (ESA), we have initiated a reprocessing of high-resolution (20 Hz) altimetry data of  
87 the Jason-1 and Jason-2 missions along coastal zones of Western Africa, Northern Europe and  
88 Mediterranean Sea. The ALES (Adaptive Leading Edge Subwaveform) retracker (Passaro et  
89 al., 2014) was applied to estimate the satellite-sea surface distance (called range) which was  
90 further combined with the X-TRACK processing chain dedicated to improve geophysical  
91 corrections at the coast (Birol et al., 2017). This allowed us to derive along-track sea level  
92 anomaly (SLA) time series (Leger et al., 2019) from which coastal sea level trends were  
93 estimated. Results show that in a number of sites, coastal sea level rates computed over a 14-  
94 year time span (2002-2016) significantly deviate from the open ocean rate within 5 km to the  
95 coast (Marti et al., 2019).

96  
97  
98  
99  
100  
101  
102  
103  
104  
105  
106  
107  
108  
109  
110  
111  
112  
113  
114  
115  
116  
117  
118  
119  
120  
121  
122  
123  
124  
125

In the present study, we focus on a particular site, Senetosa, located southern Corsica in the Mediterranean Sea ( $41^{\circ} 33'N$ ,  $8^{\circ}48'E$ ), for two reasons: (1) in this region, the computed rate of sea level rise increases significantly in the last 3-5 km to the coast, and (2) there is a Jason satellite track that crosses land at Senetosa, a calibration site for altimetry missions chosen since the launch of the Topex/Poseidon mission in 1992 and equipped for that purpose with in situ instrumentation, in particular tide gauges and GNSS antennas (Bonfond et al., 2019). This calibration site provides an independent reference to explore the near-shelf signal observed in altimetry data.

## 2. Data and method

As presented in detail in Marti et al. (2019) and Léger et al. (2019), here we use the regional X-TRACK/ALES along-track 20 Hz SLA data derived from Jason-1 and Jason-2 missions (DOI: 10.5270/esa-sl\_cci-xtrack\_ales\_sla-200201\_201610-v1.0-201910). This product is based on new ranges and new sea state bias corrections estimated using the ALES retracker (see details on the retracking methodology in Passaro et al., 2014), and further combined with the X-TRACK software developed at CTOH (Center of Topography of the Ocean and the Hydrosphere) at LEGOS (Laboratoire d'Études en Géophysique et Océanographie Spatiales). The new X-TRACK/ALES processing system first downloads from the altimetry database hosted by the French National Observations Service for altimetry called CTOH (<http://ctoh.legos.obs-mip.fr/>), all parameters needed to compute the sea level anomaly (orbit solution, altimeter ranges, instrumental, environmental and geophysical corrections). These parameters come from the Geophysical Data Records (GDRs) data sets distributed by the space agencies for the different altimetry missions. ALES range and SSB products come from TUM. Additional geophysical corrections are provided by the RADS altimeter database (<http://rads.tudelft.nl/rads/rads.shtml>) and the University of Porto (for the GPD+ wet tropospheric correction, Fernandes et al., 2015). Concerning the geophysical corrections, we used the standards defined in the ESA CCI sea level project (<http://www.esa-sealevel-cci.org/>). These are summarized in Table 1.

Parameter	Source	Jason-1 / Jason-2
Altitude	GDR	Altitude of satellite
Range	ALES/TUM	20 Hz Ku band ALES corrected altimeter range (Passaro et al. 2014)

<b>Sigma0</b>	ALES/TUM	20 Hz Ku band ALES altimeter sigma0 (Passaro et al. 2014)
Ionosphere	GDR	From dual-frequency altimeter range measurement
Dry troposphere	GDR	From ECMWF model
Wet troposphere	University of Porto	GPD+ correction (Fernandes et al. 2015)
Sea-state bias	ALES/TUM	Sea-state bias correction in Ku band, ALES retracking (Passaro et al. 2018)
Solid tides	RADS	From tide potential model (Cartwright and Taylor 1971, Cartwright and Eden 1973)
Pole tides	GDR	From Wahr 1985
Loading effect	RADS	From FES 2014 (Carrere et al. 2012)
Atmospheric correction	RADS	From MOG2D-G (Carrere and Lyard 2003) + inverse barometer
Ocean tide	RADS	From FES 2014 (Carrere et al. 2012)

126

127 *Table 1: List of altimetry parameters and geophysical corrections used in the computation of the*  
128 *coastal sea level products.*

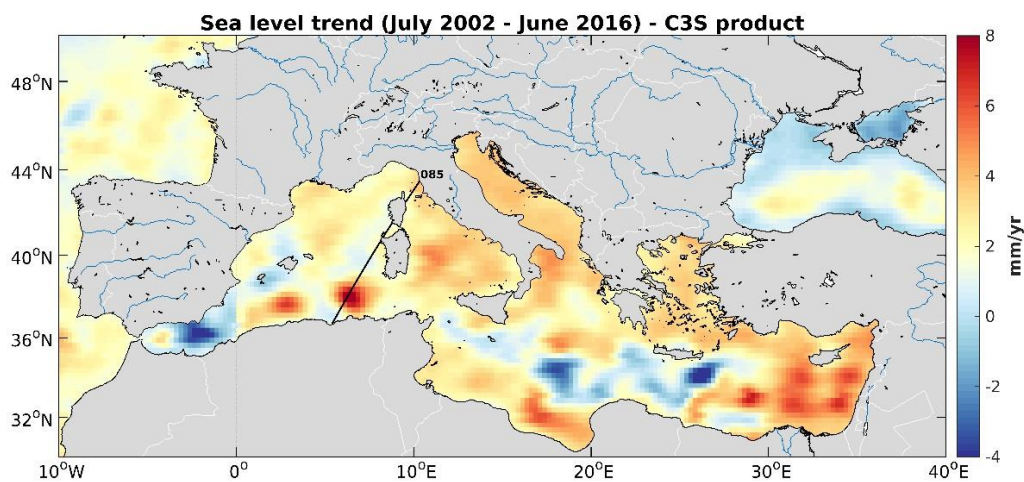
129

130 A dedicated editing strategy was further applied to eliminate noisy data. For each orbit cycle, the  
131 temporal behavior of each geophysical correction was analyzed along the satellite track. Abrupt  
132 changes were considered as spurious and removed (Birol et al., 2017). This strategy has proved to  
133 be very efficient in recovering a significant amount of valid altimeter measurements that were  
134 otherwise flagged in the standard GDR products (Jebri et al., 2016). In a second step, all corrections  
135 were recomputed at the 20-Hz high-rate using only the valid data, through interpolation/extrapolation  
136 method. The sea level data of each cycle were further projected onto fixed points along a nominal  
137 ground track and converted into SLAs by subtracting a reference mean sea surface. At this stage of  
138 the processing, a regional dataset of SLA time series with a spatio-temporal resolution of 10 days  
139 and 20Hz (~0.3 km) was produced for each Jason mission. To obtain a single multi-mission product,  
140 an inter-mission bias was estimated and removed. This was done at regional level by computing the

141 mean sea level differences between the two missions over their overlapping period (calibration  
142 phase). The resulting SLAs were further averaged on a monthly basis at every 20 Hz point and an  
143 additional editing was performed to remove outliers (details in Marti et al., 2019).

144 In this study we focus on the section of Jason track 85 located off the southwestern coast of  
145 Corsica island (Western Mediterranean Sea) (see Fig. 1).

146



147

148

149 *Fig. 1: Location of the Jason track 85 crossing Corsica at the Senetosa site (black straight line).*  
150 *The background maps shows sea level trends over 2002-2016, based on gridded altimetry data*  
151 *from the Copernicus Climate Change Service (C3S)*

### 152 3. The Senetosa calibration site

153 Since 1998, a calibration site of the Topex/Poseidon and Jason missions has  
154 operated near the Senetosa lighthouse with support from CNES (Centre National  
155 d'Études Spatiales, France), NASA (National Aeronautics and Space Administration, USA)  
156 and the Observatoire de la Côte d'Azur (France). It is equipped with different in situ  
157 instrumentation, including weather stations, several tide gauges and GNSS antenna. Since  
158 1998, this calibration site has been widely used to validate the altimetry-based sea surface  
159 height data (Bonnefond et al., 2003a,b, 2010, 2011). Fig.2 is a Google Earth image of the  
160 coast, showing the geographical configuration of the Senetosa calibration site, with the  
161 location of the tide gauges, the GNSS antenna and the Jason track. Three tide gauges were  
162 operating during our study period (M3, M4 and M5). M4 and M5, a few tens of cm apart,  
163 are located on the western part of the coastline sheltered from northwestward wind  
164 forcing. M3 at 1.7 km eastward of M4/M5 is more exposed to open sea conditions from the  
165 west.

166 Vertical land motion time series are available from the GNSS reference receiver located close  
167 to the lighthouse (G0 reference marker in Fig.2). The tide gauges have been regularly leveled  
168 relatively to the G0 reference marker with no relative motion detected so far at the millimeter  
169 level over 10 years. Trends in sea level and vertical land motions derived from these  
170 instruments at Senetosa are discussed in section 5.

171



173  
174 *Fig. 2: Google Earth image of the Senetosa calibration site. The two tide gauge sites (referred*  
175 *as M4/M5 and M3) are shown by the red dots. The G0 reference marker (G0) is indicated by a*  
176 *white square and the Jason ground track by the white straight line.*

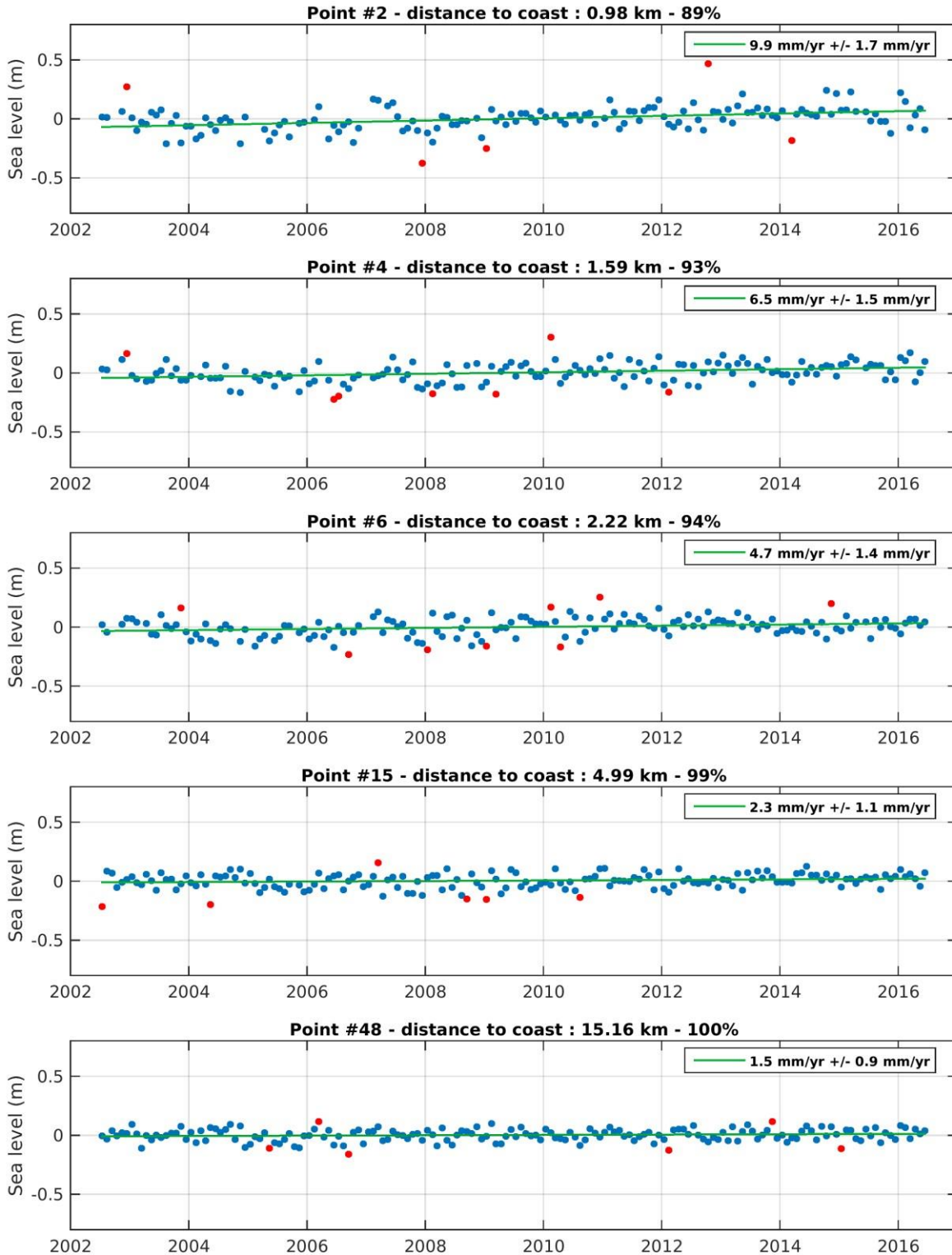
177  
178

## 179 **4. Analysis of the coastal sea level trends off Senetosa**

### 180 **4.1 Coastal sea level trends derived from altimetry data**

181 Following the data processing described above, we focus on monthly SLA time series sampled  
182 at 20 Hz (~350 m in the along-track direction), from 15 km offshore to the coastline. Examples  
183 of along-track SLA time series at coastal points, located at 1 km, 1.6 km, 2.2 km, 5 km and  
184 15 km from the coast respectively, are shown in Fig.3.



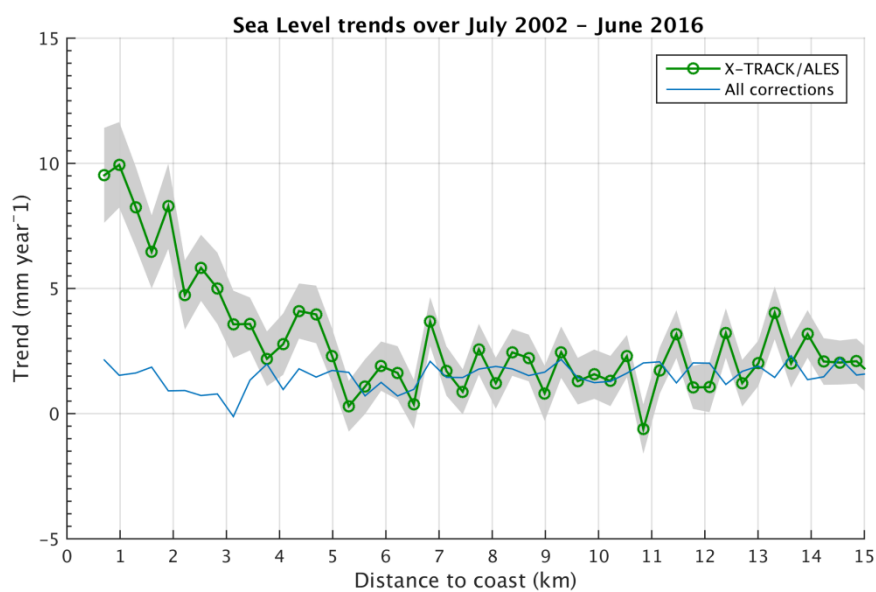


190 *Fig. 3: Examples of sea level anomalies time series for 20-Hz points located at different*  
 191 *distances from the coast. The distance to coast, percentage of valid data and sea level trends*  
 192 *are indicated on each plot. The green curve is the regression line adjusted to the data. The*  
 193 *red points on the time series correspond to outliers detected using a simple 2-sigma filter*  
 194 *(sigma corresponding to the SLA standard deviation). These are not considered to compute*  
 195 *the regression line.*

196  
197  
198  
199

200 For each 20 Hz point, we have then computed the regression line of the resulting SLA time  
201 series and the associated standard deviation (1-sigma) based on the least squares fit, to estimate  
202 sea level trends over the study time span. Fig.4 shows the corresponding along track sea level  
203 trends as a function of distance to the coast (from 15 km offshore).

204  
205  
206  
207  
208  
209  
210  
211  
212  
213  
214  
215  
216  
217  
218  
219  
220  
221  
222  
223  
224



225

226 *Fig. 4: Altimetry-based sea level trends over July 2002-June 2016 around Senetosa as a*  
227 *function of distance to the coast . Shaded area corresponds to trend uncertainty range. The*  
228 *light blue curve is the sum of trends in individual corrections.*

229

230 As shown in Fig.4, beyond ~ 5 km from the coast towards the open sea, the trend over 2002-  
231 2016 is relatively stable and on average on the order of 2-3 mm/yr. High frequency  
232 oscillations around this value are observed between adjacent points but these are likely due to  
233 noise and we note they are of the same order of magnitude or only slightly larger than the  
234 standard deviation of trend estimates at each point (of ~1.5 mm/yr).

235 As also shown in Fig.4, we note an almost continuous increase in the trend in the last ~4-5 km  
236 to coast. The corresponding trend uncertainties (standard deviation) are not significantly  
237 larger than offshore (<2 mm/yr).

238

## 239 4.2 Robustness of the computed coastal trends

240 In coastal areas, precision of sea surface height from altimetry is limited by inaccuracies in  
 241 some of the applied geophysical corrections (including sea-state bias, wet tropospheric  
 242 correction, dynamical atmospheric correction and ocean tides) and from the distorted shape of  
 243 the radar waveforms as the satellite approaches land (Vignudelli et al., 2011 and Cipollini et al.,  
 244 2018).

245 The corresponding altimetry measurements are often discarded by the processing chains or  
 246 flagged in the data sets as potentially erroneous, leading to low confidence sea level  
 247 trend estimates near the coastline. These estimates can also be impacted by the lower  
 248 percentage of valid data in the coastal zone, as well as by the uncertainty in the bias estimate  
 249 between the two successive missions Jason-1 and Jason-2. In order to check whether the sea  
 250 level trend increase close to the coast reported in section 4.1 is associated to one of these  
 251 factors, each of them is independently examined.

252

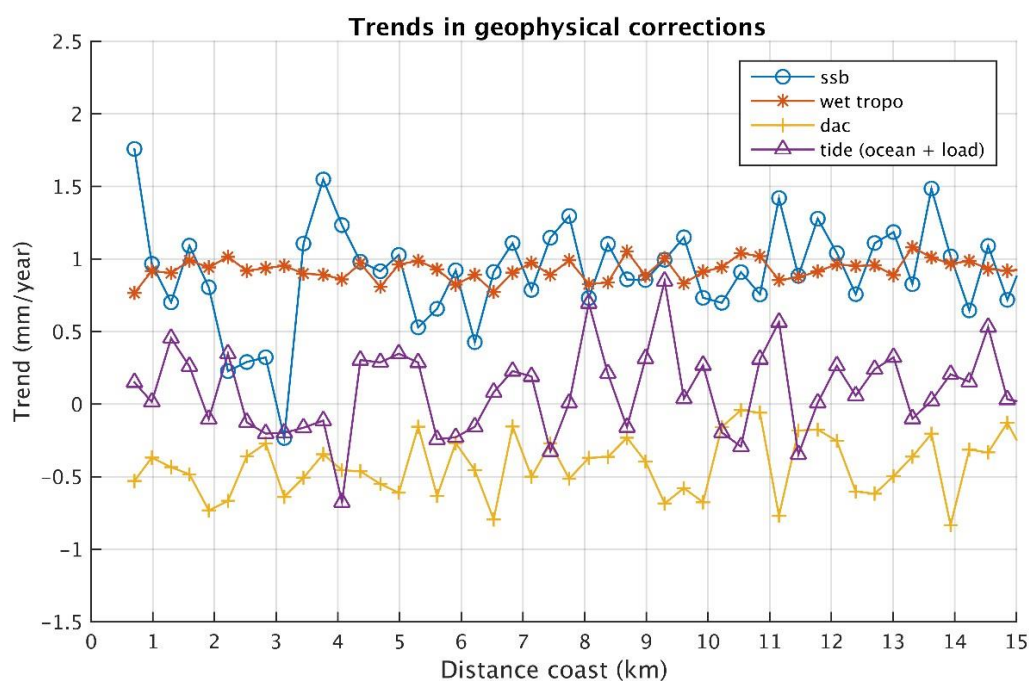
### 253 4.2.1 Coastal errors in the geophysical corrections

254 We first computed and plotted the geophysical correction trends against distance to the coast  
 255 for the sea-state bias (ssb), wet atmospheric correction, atmospheric loading (called DAC-  
 256 dynamic atmospheric correction-) and ocean and loading tide correction (Fig.5).

257

258

259



260

261  
262  
263  
264

265 *Fig. 5: Trends in the geophysical corrections (sea state bias/ssb, wet tropospheric correction,*  
266 *dynamic atmospheric correction/dac, ocean tide plus ocean loading tide) as a function of*  
267 *distance to coast. Note that the vertical scale is different from Fig.4.*

268

269 Trends in the geophysical corrections are rather small and their amplitude in the range +/- 1  
270 mm/yr, except for the ssb that shows a larger trend within 4 km to coast, but always less than  
271 2 mm/yr. It is worth mentioning that the ssb is a function of significant wave height (SWH)  
272 and backscatter coefficient (both related to wind speed). In the ALES retracking the ssb is  
273 recomputed for each 20-Hz point. So a trend in ssb may be due to either a different behavior  
274 of the SWH and wind speed at the coast, or to changes in backscatter properties.

275 The sum of these geophysical correction trends is plotted in Fig.4 (blue line). Even if the  
276 geophysical corrections, and especially the ssb, are more uncertain close to the coast, Fig. 4  
277 suggests that the continuous increase in the sea level trends observed in the last ~4 km to the  
278 coast may not be due to trends in the geophysical corrections. It remains that the empirical  
279 formulation used for the ssb correction may not be valid close to the coast where waves could  
280 have a different behavior compared to the open sea. This will be discussed in section 6.1.

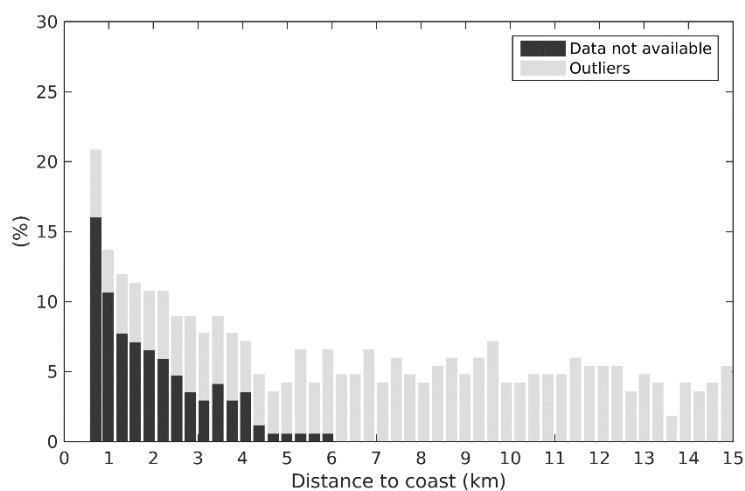
281

#### 282 4.2.2 Coastal changes in the percentage of valid data

283 We next examined the possible impact on the trend estimation of the decrease in valid data in  
284 the last 3-4 km to coast. The original percentage of valid data at each 20-Hz point decreases  
285 with distance to the coast, as shown in Fig.6. We resampled the along-track sea-level records  
286 keeping only the 80% of data common to all along track positions at a given time.

287

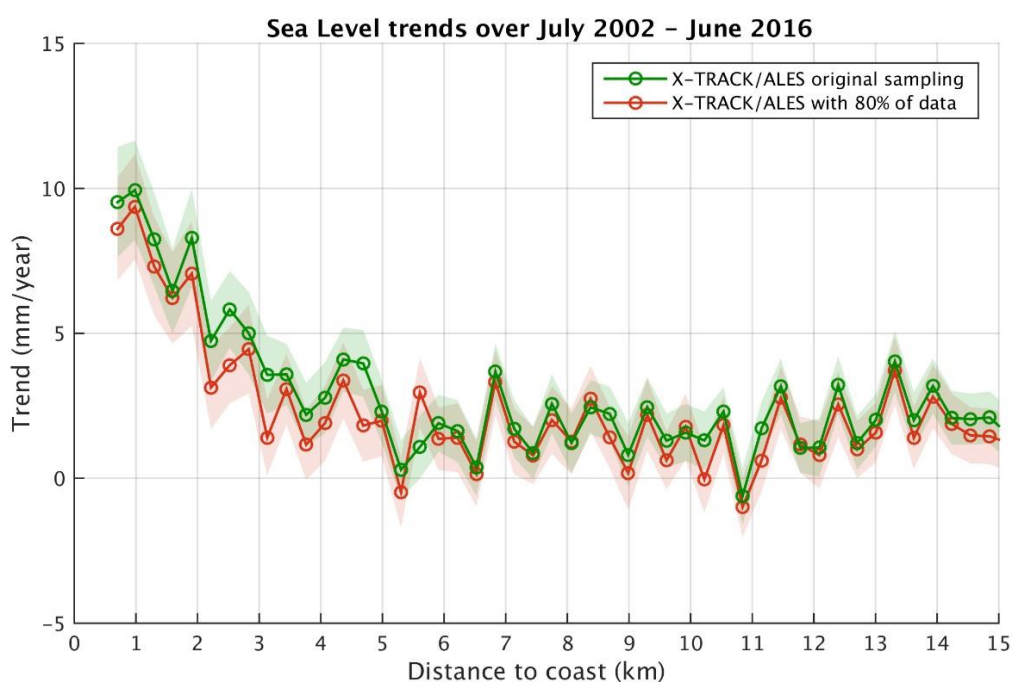
288



289  
 290  
 291  
 292  
 293  
 294  
 295  
 296  
 297  
 298  
 299  
 300

*Fig. 6: Percentage of missing points for the original data set.*

The along-track sea level trends were recomputed with the new sampling (80% of the original data kept) (Fig.7). For comparison, in Fig.7 we superimpose the trends computed with the original sampling. Trends compare well in both cases. Even if the trend values are slightly lower in the band 0-5 km, keeping only 80% of the valid data does not change significantly the coastal trend behavior. We conclude that the lower amount of valid near-shore altimetry data does not explain the trend increase observed as the distance to the coast decreases.



301

302

303

304 *Fig. 7: Sea level trends as a function of distance to the coast with the original data set (green*  
305 *curve) and new sampling (80% of original data kept; red curve).*

306

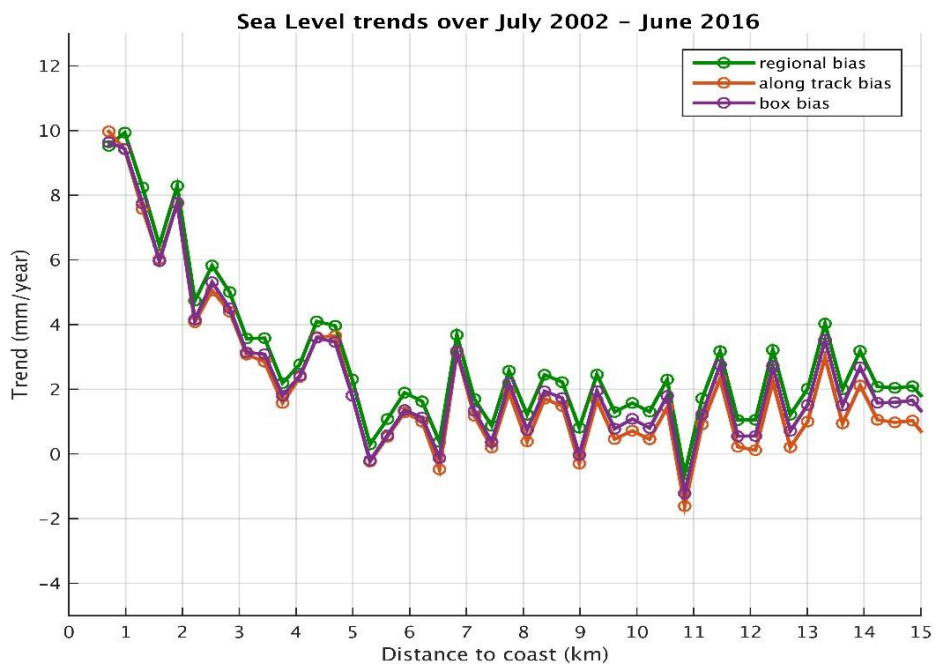
307

#### 308 4.2.3 Effect of intermission bias estimation

309 As discussed in detail in Marti et al. (2019), in the X-TRACK/ALES sea level product, the  
310 bias applied to combine the Jason-1 and Jason-2 data in a single sea level time series was  
311 estimated at a regional scale. In the case of our study region, it was estimated over the whole  
312 Mediterranean Sea. In order to investigate a possible impact of this approach on the sea level  
313 trend estimates, we tested other bias calculation methods. We first recomputed the  
314 intermission bias along the Jason track 85 (using only measurements of this particular track).  
315 In another test, the bias was computed from data included in a 1x1 degree box around the  
316 Senetosa site. The sea level trends derived from the corresponding Jason-1 and Jason-2 time  
317 series are shown in Fig. 8a for these two cases, superimposed to the regional bias case shown  
318 in section 4.1. Here again, we can see that there is almost no difference between the results of  
319 the three approaches, indicating that inadequate intermission bias estimate does not explain  
320 the coastal trend increase. To complete these tests, we also recomputed SLA trends as a  
321 function of distance to coast using as reference a local geoid computed for altimetry mission  
322 calibration purposes (P. Bonnefond, personal communication). Fig.8b shows the geoid profile  
323 together with the along-track mean sea surface computed with the altimetry data, as a function  
324 of latitude. Both references compare well. Thus, as expected, exactly the same trend increase  
325 behavior as a function of distance to coast is observed when the reference geoid is used  
326 (figure not shown as it is similar to Fig.4). We conclude that the reference has no impact on  
327 the computed trends.

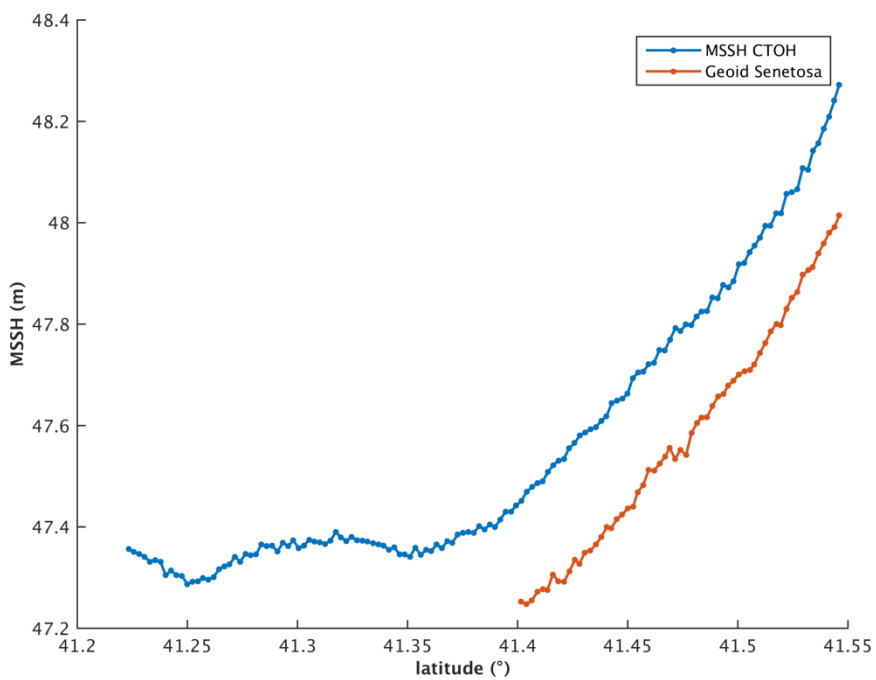
328

329 (a)  
330  
331



332  
333  
334  
335  
336

337 (b)  
338  
339  
340

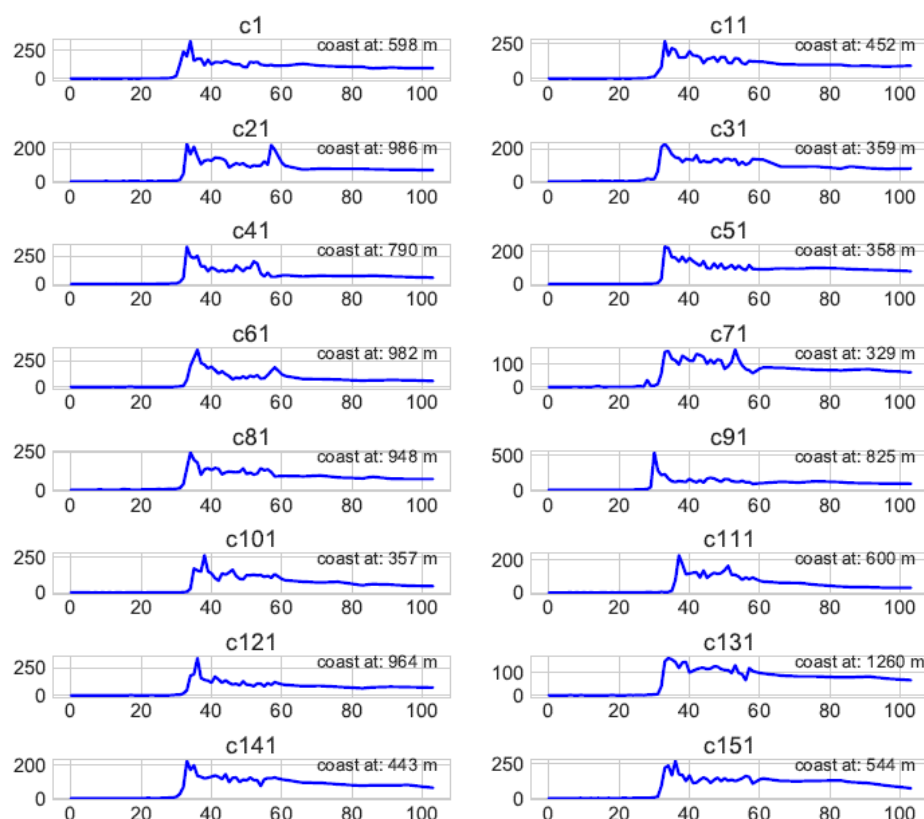


341  
 342  
 343  
 344  
 345  
 346  
 347  
 348  
 349  
 350  
 351  
 352  
 353  
 354  
 355  
 356

*Fig.8: (a) Sea level trends as a function of distance to the coast for three different intermission bias estimates. (b) Geoid and altimetry-based along-track mean sea surface profiles as a function of latitude.*

#### 4.2.4 Coastal altimetry waveforms and range values near Senetosa

In another series of tests, we examined the shape of the radar waveforms at 20 Hz points as a function of distance to coast, considering a few Jason cycles taken at random. An example is shown in Fig. 9 for a point located between the coast and 2 km offshore. Fig.9 shows that at the Senetosa site, the leading edge of the coastal radar echo is generally well defined, suggesting that a robust determination of the range is possible very close to the coast.



357  
 358  
 359  
 360  
 361  
 362  
 363  
 364

*Fig. 9: Observed radar waveforms at points close to the coast for a series of Jason cycles (numbers on each plot refer to cycle number).*

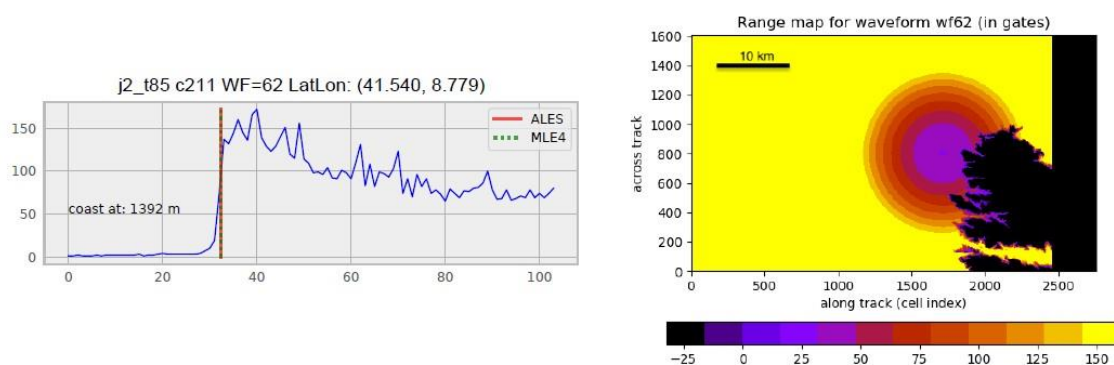
To investigate this further, we tried to assess the reliability of successive 20-Hz ALES-based range data very close to the coast. The waveform amplitude represents the radar power as a



365  
 366 function of time. For Jason-2, time is discretized into 104 successive ‘gates’. Knowledge of  
 367 the orbit and radar footprint allows by simple geometric analysis to associate a point on  
 368 ground (pixel) to a given gate. A numerical simulation has been performed for that purpose  
 369 (assuming flat land) in order to produce range maps for the Jason track 85, with the goal of  
 370 precisely locating the point on ground corresponding to the measured waveform. This is  
 371 illustrated on Fig. 10a and Fig. 10b, showing the geographical configuration and associated  
 372 radar waveforms for two range measurements located at 0.53 km and 1.4 km distance from  
 373 coast. The range measurement deduced from the waveform corresponds to the center of the  
 374 circle representing the radar footprint on the range map.

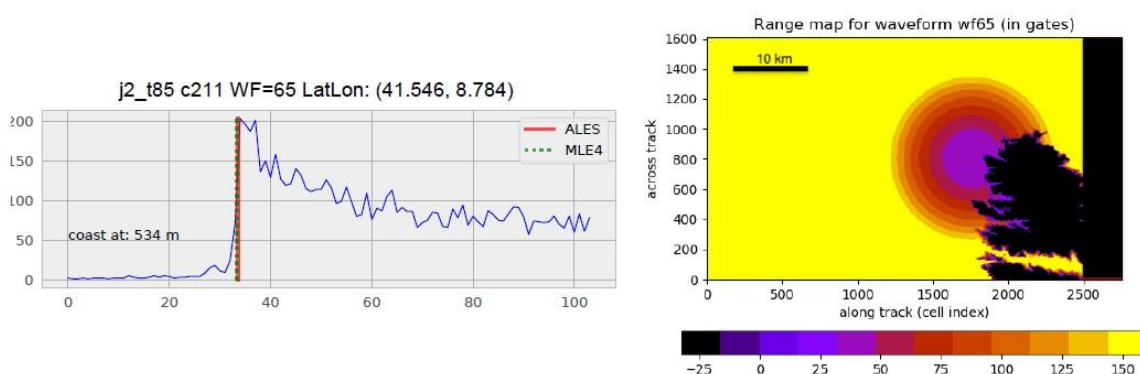
375  
 376  
 377  
 378  
 379

(a)



380

(b)



383  
 384

385 *Fig. 10: (a) Radar waveform as a function of gate number (left) and configuration of the*  
 386 *radar footprint on ground (right) at 1.4 km from coast. (b) Same as (a) at 0.5 km from coast.*

387  
 388

389 Although these simulations represent an ideal case of smooth sea state and flat land, Fig.  
 390 10a,b shows that even at the closest point to coast (0.5 km), the leading edge of the return

391  
392 waveform still corresponds to a reflection of the radar signal on water. This suggests that it is  
393 theoretically possible to retrieve valid sea level information up to 0.5 km to the coast. One  
394 may argue that because the land at Senetosa has some elevation, the real radar echo is partly  
395 contaminated by land reflection at distances larger than the theoretical footprint, even if there  
396 is no wave. However, considering that the real waveform has a leading edge, and that  
397 the retracker is able to follow it, we conclude that the trends reported on successive 20-Hz  
398 points are not spurious. Besides, if the retracker was corrupted by inhomogeneous backscatter  
399 properties within the satellite footprint, these should be random (e.g., Passaro et al. 2014).  
400 Finally, 20-Hz waveforms being independent samples, if the retracker is wrong and produces  
401 spurious trends, the latter also would be random. Thus, we should not see a continuous trend  
402 increase over several consecutive points.

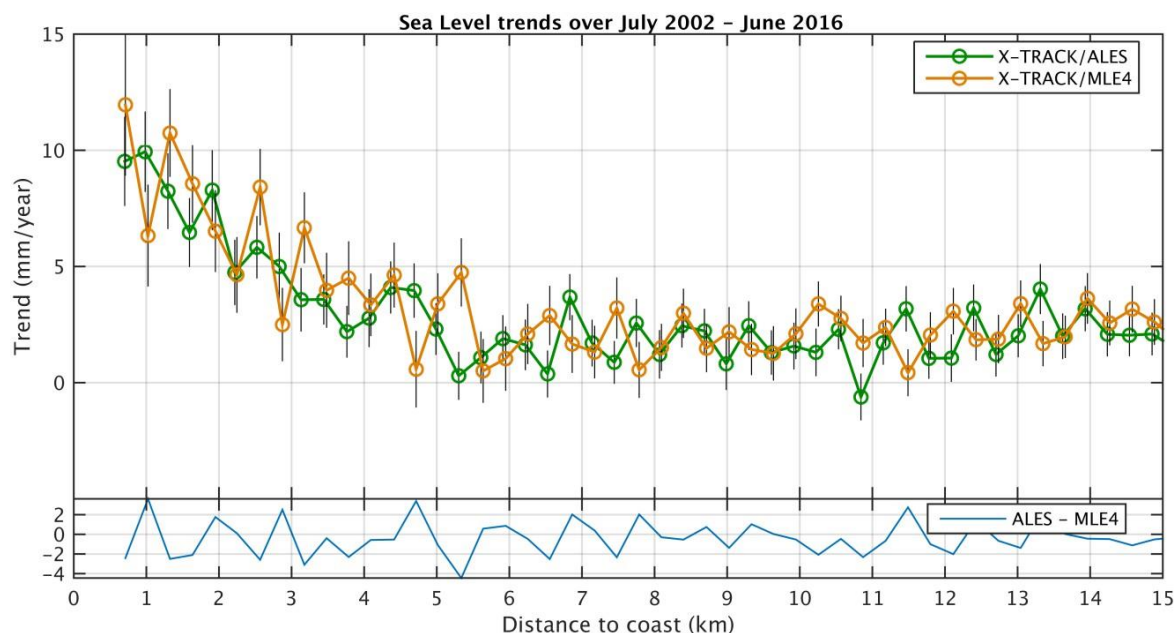
403

#### 404 4.2.6 Comparison between ALES and MLE4 retrackers

405 Finally, we performed the same analysis (computation of sea level trends as a function of  
406 distance to the coast) using SLA data computed with the classical MLE4 retracker (used for  
407 the standard Geophysical Data Records production,  
408 [https://www.aviso.altimetry.fr/fileadmin/documents/data/tools/hdbk\\_tp\\_gdrm.pdf](https://www.aviso.altimetry.fr/fileadmin/documents/data/tools/hdbk_tp_gdrm.pdf)). MLE4-  
409 based trends over the 14-year time span are shown in Fig. 11, on which are superimposed the  
410 ALES-based trends, for comparison. We note that MLE4 gives noisier results than ALES,  
411 especially at distances less than ~5 km to the coast, but the increase in trends in the last ~4-5  
412 km to the coast is still well visible. This clearly means that the trend increase is not an artifact  
413 due to the use of the ALES retracker.

414

415



416

417

418

419

420 *Fig. 11: Sea level trends as a function of distance to the coast for MLE4 (orange dots) and*  
 421 *ALES (green dots)-based SLA data. Vertical bars correspond to trend errors (1-sigma). The*  
 422 *light blue curve at the bottom of the panel represents the difference between ALES-based and*  
 423 *MLE4-based trends.*

424

425

426

427

428

429

430

431

432

433

434

435

436

437

438

439

440

441

To summarize, from all the tests presented above, we can conclude that the increase in altimetry sea level trend observed in the last 4-5 km to the coast is not correlated with errors in the geophysical corrections, is not explained by the loss of valid data, nor the presence of spurious waveforms or by the intermission bias. Furthermore, the calculated trends are robust to change in retracker, since instead of using ALES, we also used the standard high-frequency MLE4 retracker. The corresponding time series still show the same trend behavior (although with noisier results).

## 5. Comparison with the sea level trend derived from tide gauges records

It is very classical to validate altimetry-based sea level data by comparing with tide gauge records. The availability of tide gauge records at the Senetosa site is a good opportunity to do so. Tide gauge data have been provided by the Observatoire de la Côte d'Azur (Géoazur laboratory) and downloaded from [www.aviso.altimetry.fr/en/data/calval/in-situ/absolute-calibration/download-tide-gauge-data.html](http://www.aviso.altimetry.fr/en/data/calval/in-situ/absolute-calibration/download-tide-gauge-data.html). The high-frequency tidal signal and the atmospheric forcing effect have been removed (using the same DAC correction as for the

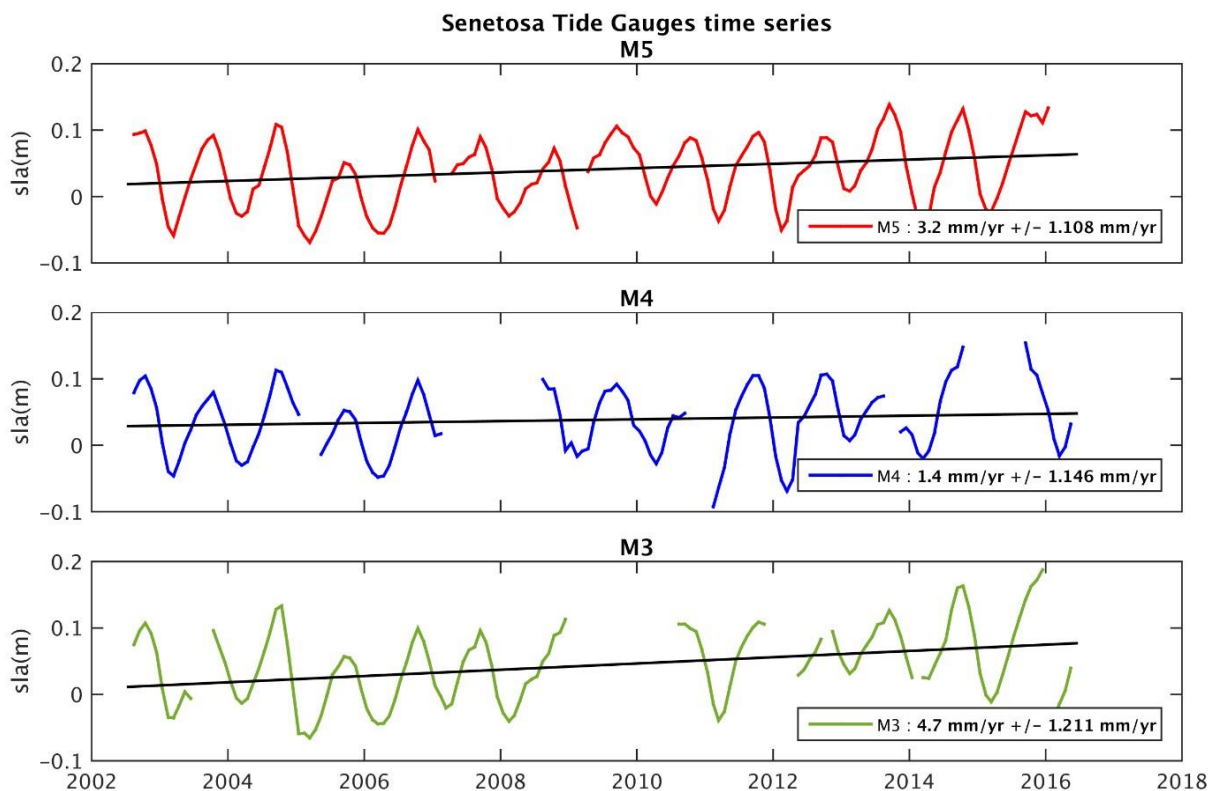
442

443 altimetry data). The time series have been further smoothed on a monthly basis. The  
 444 corresponding tide gauge time series over 2002-2016, for the M3, M4 and M5 tide gauges, are  
 445 shown in Fig. 12a and 12b, with and without the seasonal cycles.

446

447  
 448

(a)

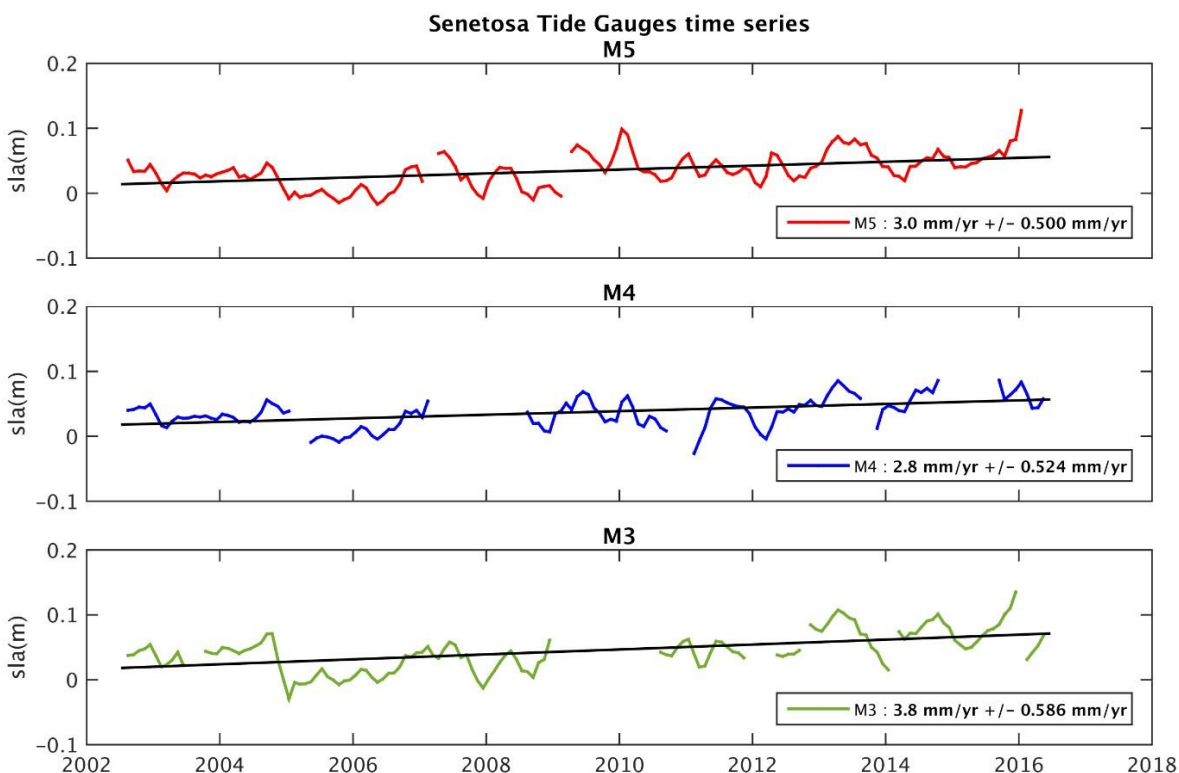


449

450

451

(b)



452

453  
454  
455  
456  
457  
458  
459  
460  
461  
462  
463  
464  
465  
466  
467

*Fig. 12: Sea level time series based on in situ tide gauges measurements at the M3, M4 and M5 sites over 2002-2016. (a) With the seasonal cycle. (b) Without the seasonal cycle.*

From these time series, we computed linear trends over the same period as for the altimetry data. These are gathered in Table 1 for the two cases (with and without the seasonal cycle). In Bonnefond et al. (2019), it was shown that when making differences between tide gauges sea level measurements, there is no systematic trend between the tide gauge time series since 2001 (below 0.1 mm/yr), well within the trend uncertainties. The GNSS-based vertical land motion (VLM) at Senetosa (estimated in Bonnefond et al., 2019) is also shown. VLM is small at Senetosa, less than 0.3 mm/yr.

Tide Gauge	Tide gauge trend (mm/yr) (with seasonal cycles)	Tide gauge trend (mm/yr) without seasonal cycles	GNSS VLM (2003-present) (mm/yr)
M3	4.7 +/- 1.2	3.8 +/- 0.6	0.28 +/- 0.05
M4	1.4 +/- 1.1	2.8 +/- 0.5	0.28 +/- 0.05
M5	3.2 +/- 1.1	3.0 +/- 0.5	0.28 +/- 0.05

468

*Table 1: Relative sea level trends (mm/yr) recorded by the M3, M4 and M5 tide gauges (estimated with and without the seasonal cycles) as well as the GNSS-based vertical land motion (mm/yr) at the Senetosa site.*

472

The M4 time series displays several gaps over the study period. In addition, the record (seasonal cycle not removed, Fig. 12a) shows a large positive anomaly in 2015, not seen by M3 neither M5. M3 has also a large gap in 2009/2010, as well as other gaps 2012 and at the end of the record. A suspect drop is also visible in 2005 on Fig. 12b (seasonal cycle removed). Thus the M5 record seems the most reliable, even if the trends from M3 and M4 are close to M5 (see Table 1). The computed (relative) sea level trend (uncorrected for the VLM) is on the order of 2.8-3.8 mm/yr over the study period (seasonal cycle removed). If the GNSS VLM trend is accounted for, this range becomes 3.1-4.1 mm/yr. This value is significantly less than the altimetry-based sea level trends reported here in the last 4-5 km to the coast. On the other hand, the tide gauge trend agree well with the altimetry-based trends reported at distances greater than > 4 km from coast. While the reported altimetry-based sea level trend increase may disqualify our retracked sea level data in the vicinity of the coast, in

484

485  
486 the next section we discuss the possibility that some coastal processes affect sea level in a  
487 band of a few km from the coast while being attenuated very close to the shore where the tide  
488 gauges (in particular M5) are located. .

489

## 490 **6. Small scale coastal processes**

491 Compared to deep-ocean sea level, sea level close to the coast can be impacted by various  
492 small-scales processes resulting from the morphology of the coastline, the depth of the  
493 continental shelf, the presence of a river estuary, etc. (Woodworth et al., 2019). Thus coastal  
494 sea level may significantly differ from open ocean sea level over a large range of temporal  
495 scales. In terms of trends, the open ocean sea level essentially results from processes affecting  
496 the global mean sea level (mean ocean thermal expansion, land ice melt and land water  
497 storage changes) (e.g., WCRP, 2018) and the superimposed regional variability (regional  
498 changes in ocean thermal expansion, atmospheric loading and fingerprints due to the solid  
499 Earth response to changing ice mass loads; Stammer et al., 2013). At the coast, in addition of  
500 these two contributions, local variations in other processes may cause additional small-scale  
501 sea level changes at interannual to decadal time scales, such as trapped Kelvin waves,  
502 upwelling/downwelling effects, eddies, wind-generated waves and swells, shelf currents, water  
503 density changes related with river runoff in estuaries (see Woodworth et al., 2019 for a detailed  
504 discussion on forcing factors affecting sea level changes at the coast). Note that we do not  
505 discuss vertical land motion here since our objective is to understand the observed change  
506 in ‘geocentric’ sea level as measured by satellite altimetry.

507 In the case of Senetosa, river runoff and trapped Kelvin waves are not supposed to affect  
508 coastal sea level. Could other processes like trends in wind-generated waves and coastal  
509 currents explain the slow increase in sea level trend towards the coast? These are discussed  
510 below.

511

### 512 **6.1 Effect of waves on SLA and SSB**

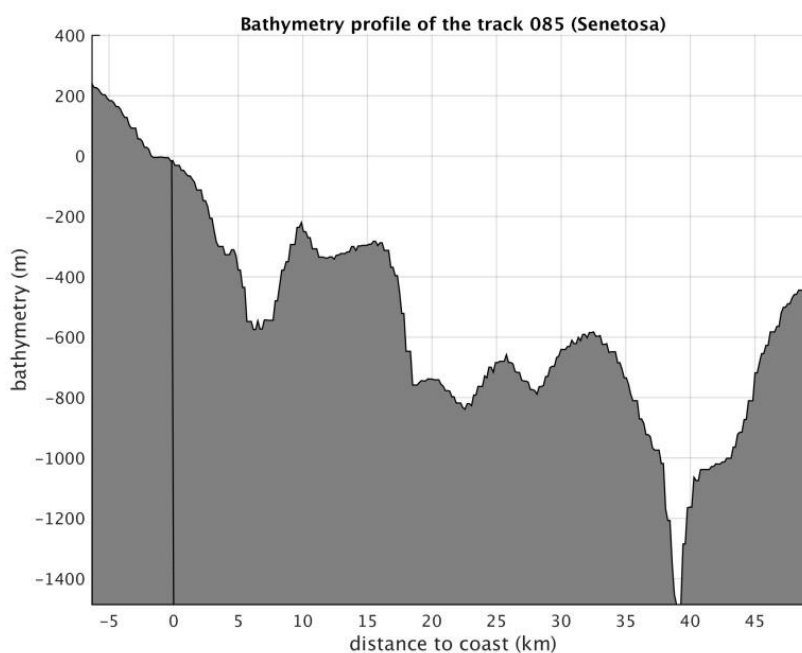
513 We first discuss the effect of waves. The contribution of wind-generated waves to coastal sea  
514 level changes has been investigated in a number of recent studies (e.g., Melet et al., 2018,  
515 Dodet et al., 2019). As thoroughly discussed in Dodet et al. (2019), wind-generated waves  
516 have the capability to significantly change sea level variations at the coast, even at the time  
517 scales of interest here. The shoaling and breaking of waves in the shelf shallow waters raises  
518 the mean water level in the so-called near-shore and surf zones (last ~1 km to coast), a

519

520 process called wave set-up. Wave set-up is proportional to offshore significant wave height,  
 521 and if the latter displays a temporal trend due to a trend in wind forcing, it may cause a sea  
 522 level trend in the coastal zone.

523 The relationship between offshore wave height and wave set-up is known empirically only  
 524 (Dodet et al., 2019). To first order, wave set-up is related to offshore SWH, wave period and  
 525 beach slope. The bathymetric profile along the Jason track 85 (from 45 km offshore to coast)  
 526 is shown in Fig. 13. We note an abrupt increase of more than 500 m in the last 5 km to coast,  
 527 corresponding to a slope of 0.1.

528



529

530

531 *Fig. 13: Bathymetric profile (meters) along Jason track 85 from 45 km offshore to coast*

532

533

534 If the bathymetric slope near Senetosa is known, it is not the case for other parameters  
 535 involved in the relationship between SWH and wave set-up. This is the case in particular for  
 536 beach soil characteristics, sediment size, etc. A large variety of formulations have been  
 537 proposed for this relationship, based on in situ observations collected at different coastal sites  
 538 (e.g., Dodet et al., 2019). However, these are not necessarily applicable to our study case as  
 539 some local beach parameters are not known. But it is generally assumed that wave set up does  
 540 not exceed 20% of SWH. Thus, as a preliminary approach, we analyzed offshore SWH data  
 541 only, in order to highlight their temporal variability over our study time span.

542 For that purpose we considered wave field data from the ERA5 reanalysis  
 543 (<https://www.ecmwf.int/en/forecasts/datasets/reanalysis-datasets/era5>). The ERA5 reanalysis

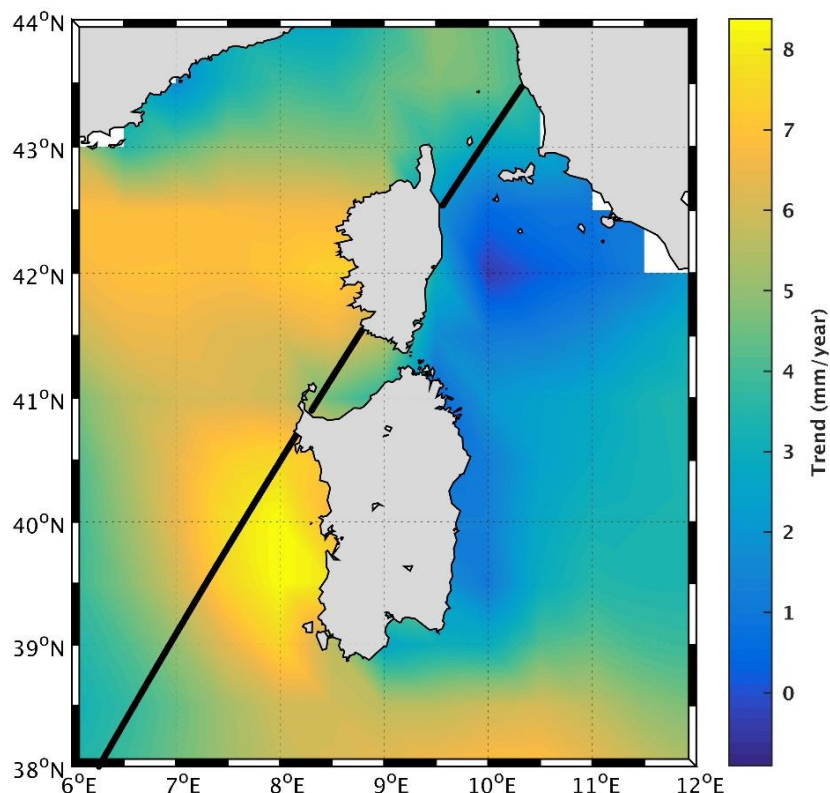
544

545 provides gridded SWH time series at monthly interval, from 1979-present, thus covering our  
 546 study period. The grid size resolution is 0.5 degree. Using this data set, we computed 2-D  
 547 SWH trends over 2002-2016, shown in Fig. 14. We note high positive wave height trends  
 548 west of Corsica and Sardinia over this period. Along the Jason track 85, in the vicinity of  
 549 Senetosia, the trend is on the order of 5 mm/yr. Note that we also computed the wind trend using  
 550 the same ERA5 reanalysis gridded data over the same period (2002-2016). The map (not shown)  
 551 displays positive trends in wind south of Corsica, although with smaller amplitude than along  
 552 the western coast of Sardinia, like the wave height map shown in Fig.14.

553 From the above discussion, we deduce that wave set up would not contribute by more that 1  
 554 mm/yr to the coastal sea level trend. Noting in addition that wave set up would affect sea level  
 555 in the close vicinity of the coast only (i.e., not over 4-5 km distance, X. Bertin, and J. Wolf,  
 556 personal communications), it is very unlikely that wave set up can explain the reported coastal  
 557 sea level trend.

558

559



560

561

562 *Fig. 14: Wave height trends (in mm/yr) over 2002-2016 in the western Mediterranean Sea*  
 563 *(data from ERA5 reanalysis)*

564

565 We further investigated the effect of waves on the ssb correction, hence on SLAs. For that  
 566 purpose, we computed the correlation between wave height time series and difference in sea

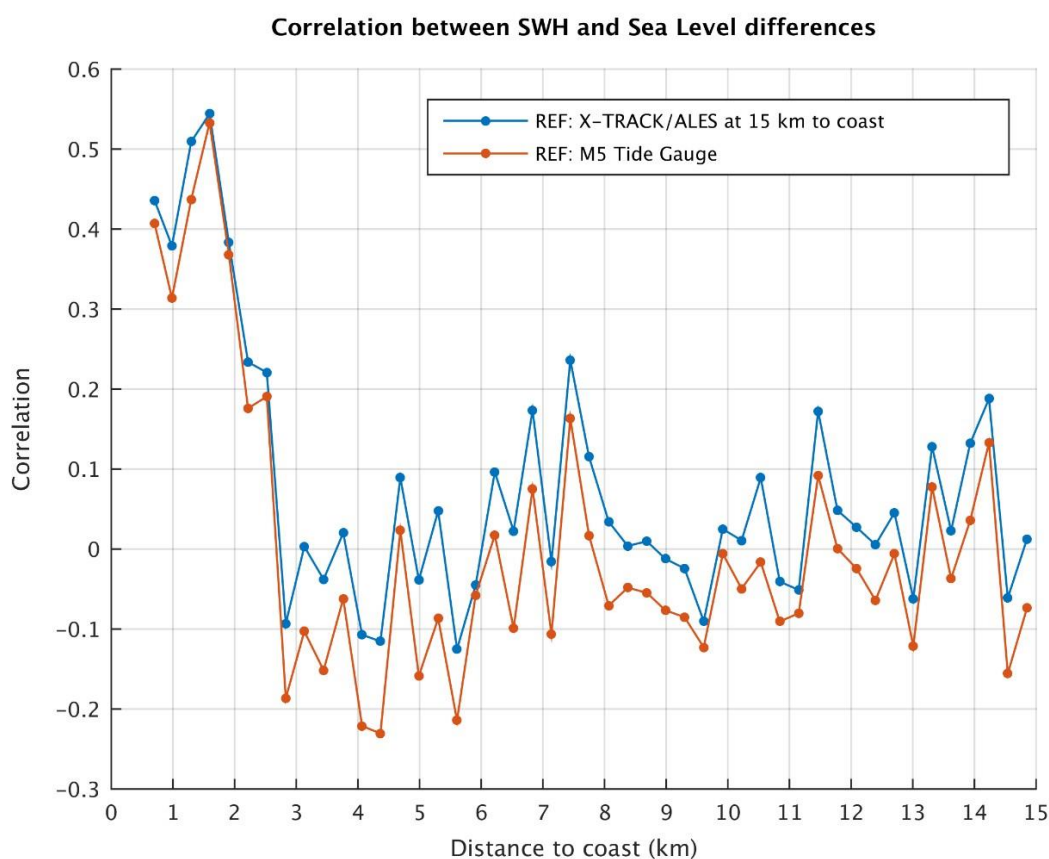


567 level between each 20 Hz altimetry point and a reference altimetry point located in the

568 open ocean (chosen here at 15 km from the coast). We consider differences in sea level  
 569 anomalies in order to remove the common ocean signal affecting sea level close to the  
 570 coast and offshore, e.g., the global mean sea level rise and its superimposed regional  
 571 variability. By computing the sea level differences between 15 km offshore and  
 572 coast, the latter large-scale sea level components are removed, leaving only  
 573 small-scale signals occurring very close to the coast. Data from the ERA5 grid  
 574 closest to Senetosa were used (the center of the considered grid point is located at 24 km from  
 575 the first valid point on the Jason track and 25 km from Senetosa). The correlation values are  
 576 shown in Fig. 15 against distance to the coast. From a distance of  $\sim 3$  km from the coast towards  
 577 the deep sea, the correlation between wave height and sea level difference is insignificant while  
 578 it clearly increases from  $\sim 3$  km to the coast. This suggests that there is a link between the  
 579 variations in waves and SLA variations in the 0-3 km domain close to land.

580 We performed the same analysis but now using the M5 tide gauge record as reference (the M3  
 581 tide gauge record having too many data gaps). This is also shown in Fig. 15. Surprisingly, we  
 582 find exactly the same behavior of the correlation coefficient, i.e., no correlation offshore  
 583 (points located at distance  $> 3$  km from coast) and an increase in correlation in the last 3 km  
 584 to the coast. This suggests that waves may affect SLA only in the domain 0-3 km from coast  
 585 but that at the tide gauge site, waves have no influence. Obviously, this could be via the ssb  
 586 correction applied to SLA data.

587  
 588



589

590

591 *Fig. 15: Correlation between the wave height (SWH) time series (from ERA5 grid mesh close*  
 592 *to Senetosa) and altimetry-based sea level difference time series between every 20 Hz point*  
 593 *and a reference point. (a) The reference time series corresponds to a point located at 15 km*  
 594 *from the coast. (b) The reference time series is the M5 tide gauge record.*

595

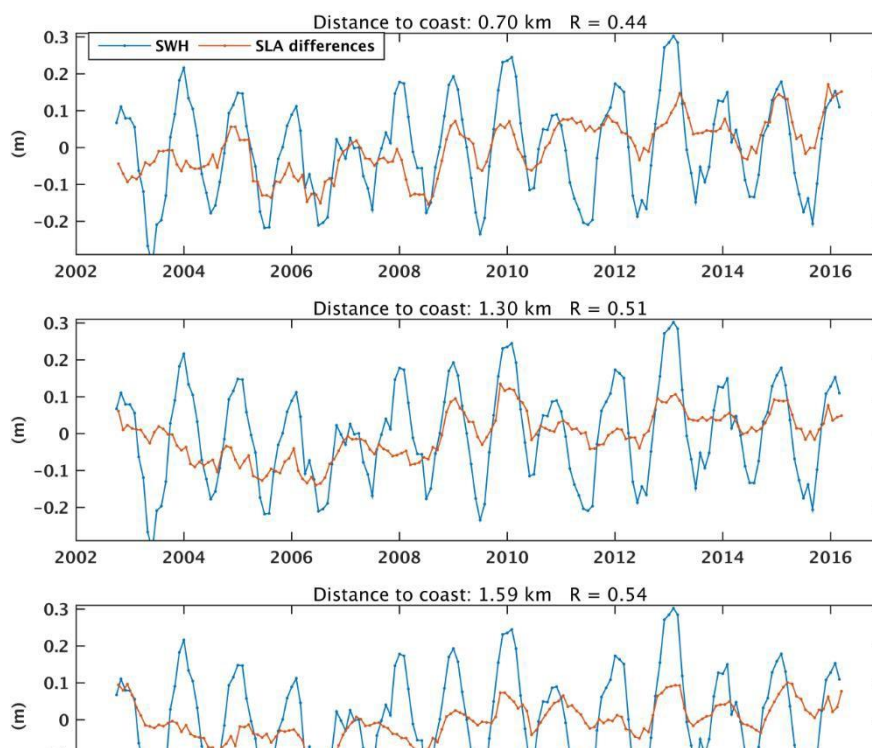
596 It has been demonstrated that applying the ssb correction to altimetry data, in particular to high-  
 597 frequency data as in this study, reduces the correlation between SWH and range (and,  
 598 consequently, SLA) (Passaro et al., 2018). The ssb correction is mainly a function of SWH: it  
 599 removes from the range estimation an effect that is directly proportional to the wave height.  
 600 This means that if this ssb correction is not applied, it has to be expected that the SLA record  
 601 will be correlated with the SWH record. To illustrate this somewhat differently, Fig. 16a shows  
 602 wave height time series superimposed to altimetry-based difference in SLA time series  
 603 (reference point at 15 km, as in Fig. 15) for a few points located in the 0-3 km domain close  
 604 to the coast and an additional point located farther from the coast. Here again, data from  
 605 the ERA5 grid closest to Senetosa have been considered for the calculation. The correlation  
 606 between SWH and difference SLA time series is indicated on each plot. We clearly see that  
 607 it is significant only for points close to the coast. Distant offshore points do not show such  
 608 a correlation. Although the correlation is dominated by the seasonal signal, Fig. 16a shows  
 609 the two time series are also correlated at interannual time scales.

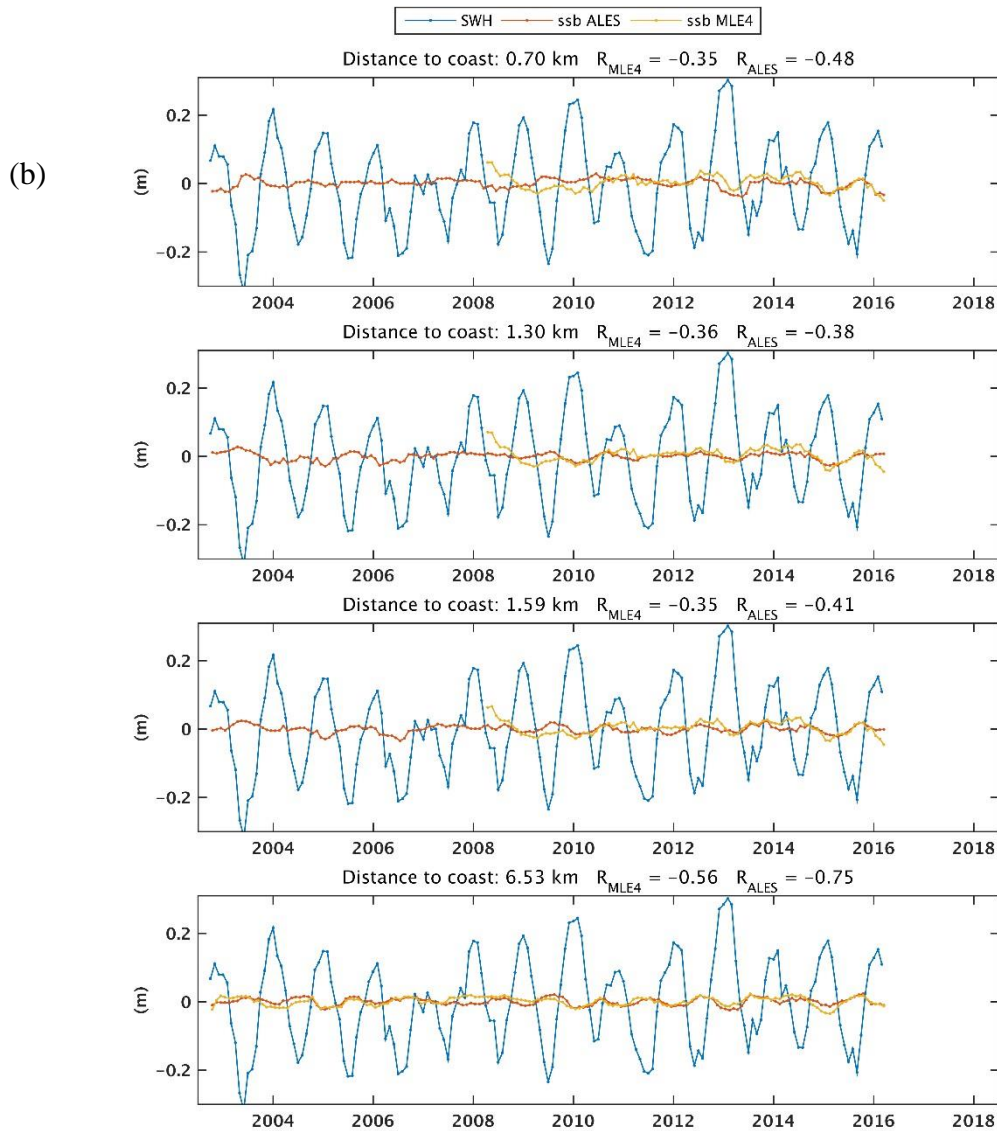
610

611 We argue that when the range close to the coast is not being properly corrected for the ssb, this  
 612 results in a correlation between ssb and SWH. To verify this, we repeated this correlation  
 613 analysis but now using the ssb correction (from both the ALES and MLE4  
 614 retrackings) instead of the SLA differences. The corresponding figure is shown in Fig. 16b.

615

616 (a)





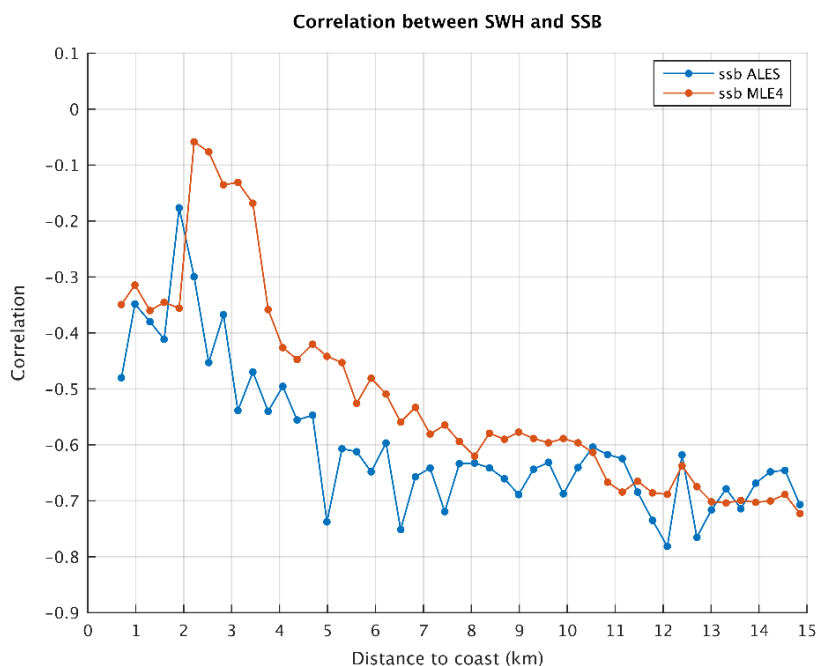
660 *Fig. 16: (a) Time series of ERA5-based wave height time series (blue curve) and of altimetry-*  
 661 *based SLA differences (orange curve) between 20 Hz points at different distances from coast*  
 662 *(indicated on each plot) and a reference point (located at 15 km). (b) same as (a) but using*  
 663 *ALES ssb instead of SLA differences. On Fig. 16b, MLE4 ssb are also shown for the Jason-2*  
 664 *time span (yellow curve).  $R$  is the correlation coefficient.*

665 As expected, ssb is correlated with SWH away from the coast, but the correlation decreases in  
 666 the last few km to the coast, suggesting that the relationship used to express the link  
 667 between ssb and SWH is less adapted in the coastal domain than in the open sea, either because  
 668 of change of wave properties (which makes the ssb model invalid) or because of a wrong  
 669 estimation of SWH very close to the coast. This is also illustrated in Fig. 17 that shows the  
 670 correlation between ssb and SWH against to distance to the coast (for both ALES ssb and  
 671 MLE4 ssb). Between 1 km

672

673 and 4 km, the correlation between SWH and ssb decreases. It is worth noting however that  
 674 the correlation remains higher for ALES ssb than for MLE4 ssb.

675



676

677

678 Fig. 17: Correlation between significant wave height (SWH) time series and ssb time series  
 679 between every 20 Hz point and a reference point.

680

681 We conclude from these tests, that the correlation between SLA and wave height at 20 Hz  
 682 points close to the coast is very likely due to imperfect ssb correction. Thus we can now  
 683 exclude any direct effect of waves (e.g., trend in wave set-up) as a candidate to explain the  
 684 SLA trend increase close to the coast. Are the reported SLA trends in the last few km to the  
 685 coast due to inadequate formulation of the relationship between SWH and ssb as the satellite  
 686 approaches the coast remains so far an open question. While we cannot exclude that the ssb  
 687 correction is imperfect close to the coast, it seems unlikely that it would produce such large  
 688 trends as those observed in the SLAs.

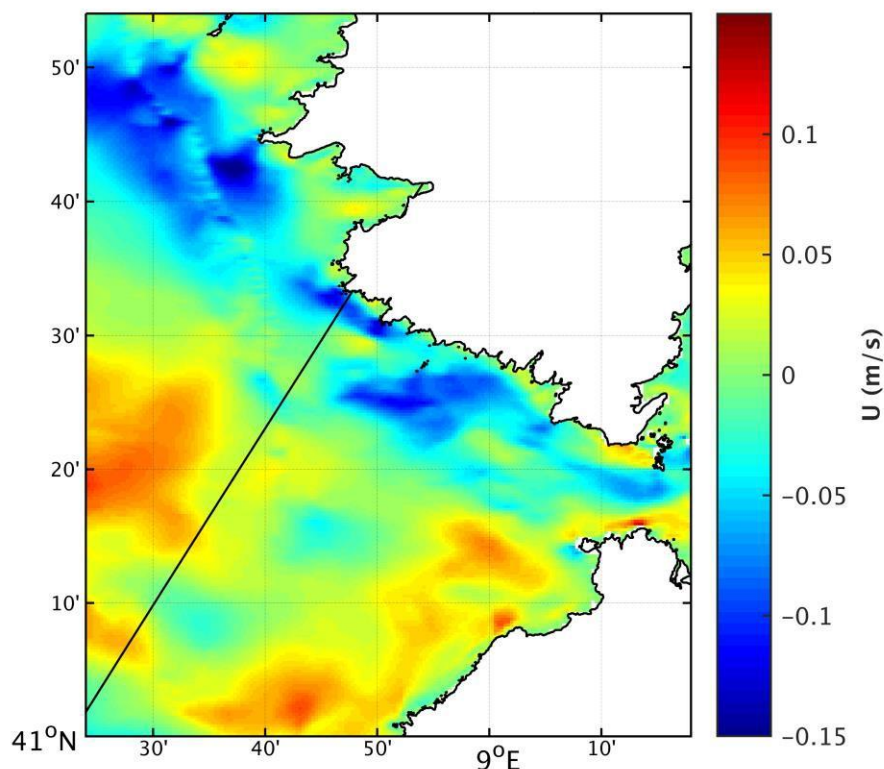
689

## 690 6.2. Effect of coastal currents and comparison with an ocean model

691 In this section we briefly address the effect of coastal currents on the SLAs. There are only  
 692 few published studies on the circulation in the Senetosa region (e.g., Bruschi et al., 1981,  
 693 Manzena et al., 1985, Cucco et al., 2012, Gerigny et al., 2015, Sciascia et al., 2019). These  
 694 indicate that the dominant characteristics of the circulation in the Corsica channel (Bonifacio  
 695 Straits) is a flow predominantly directed northward from the Tyrrhenian Sea to the Ligurian

696

697 Sea and that the water motion is mainly wind-driven. The study by Gerigny et al. (2015)  
698 based on in situ measurements collected during a cruise in 2012 and use of a high-resolution  
699 regional hydrodynamic model (MARS3D) shows that the circulation is mostly wind-driven,  
700 forced by westerly winds half of the year and strong easterly winds in winter, generating strong  
701 local currents and mesoscale structures in the western part of the channel. We have  
702 downloaded the currents data generated by the MARS3D model, a coastal hydrodynamical  
703 model developed by IFREMER (Institut Français de Recherche pour l'Exploitation de la  
704 Mer; Lazure and Dumas 2008). There is a high-resolution (400 m) version available for the  
705 Corsica region, for the years 2014 to present  
706 (<http://www.ifremer.fr/docmars/html/doc.basic.intro.html>). The model does not assimilate  
707 altimetry data nor any other type of data. Because this dataset has only 2.5 years of overlap with  
708 our study period, we cannot compute trends. However, to gain some insight on the circulation  
709 configuration, we examined the currents pattern over the year 2014. In agreement with the  
710 literature, we observed a strong zonal current during the winter months close to Senetosa. An  
711 example of the zonal component of the barotropic current south of Corsica is shown in Fig.18  
712 for January 2014. We note a clear westward current along the Senetosa coast starting at ~4 km  
713 from the coast. It is also worth noting that it does not extend to the shoreline, thus may not  
714 influence tide gauge measurements.  
715



716

717

718 *Fig.18: Barotropic current (zonal component) for January 2014 based on the MARS3D*  
 719 *hydrographic model. Blue color means westward current. The Jason track (black line) crosses*  
 720 *this current at 4 km from the coast.*

721

722 We interpolated these current data (for January 2014) along the Jason track. This is shown in  
 723 Fig.19 against distance to the coast. The current intensity is close to zero at distances >5km from  
 724 the coast. In the last 5 km to the coast, there is a steep intensity increase, exactly over the same  
 725 distance range as the SLA trend increase. Since the model resolution is ~400m, i.e., about the  
 726 same resolution as the 20 Hz along-track SLAs, we find this result highly promising.

727

728

729

730

731

732

733

734

735

736

737

738

739

740

741

742

743

744

745

746

747

748

749

750

751

752

753

754

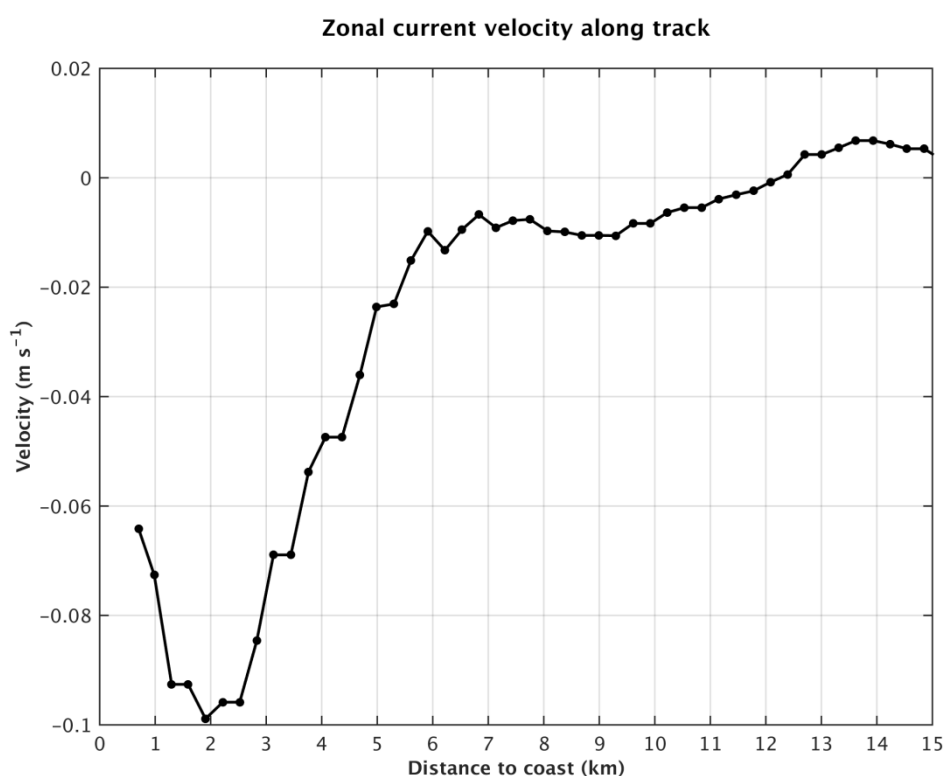
755

756

757

758

759



752 *Fig.19: Barotropic current (zonal component) for January 2014 based on the MARS3D*  
 753 *hydrographic model interpolated along the Jason track, as a function of distance to the coast.*  
 754 *Negative values mean westward current.*

755

756 Of course, we cannot extrapolate backward in time nor offer any solid conclusion so far. But we  
 757 cannot exclude that the observed sea level trend increase is linked to an increase in intensity of  
 758 this winter current during our study period. This obviously will need much deeper investigation,  
 759 at least over the time span of availability of the model data.

760

## 761 **7. Conclusion**

762 In this study, we have investigated the differences between coastal and deep ocean sea level  
763 changes at the Senetosa site, using new ALES-based retracked sea level data from the Jason-1  
764 and Jason-2 missions. We indeed observe a slow increase in sea level trend at short ( $< \sim 4$ -5  
765 km) distance from the coast compared to offshore. A series of test shows that this behavior  
766 does not result from artifacts due to spurious trends in the geophysical corrections applied to  
767 the altimetry data, decreasing percentage of valid data, or errors in the intermission bias nor  
768 errors in range estimates due to distorted radar waveforms.

769 While the paper was in review, an update of the results presented above has been recently  
770 performed extending the SLA time series with Jason-3 data up to June 2018 (coastal trends based  
771 on Jason-1, 2 and 3 over 2002-2018 at several hundreds of coastal sites located in six different  
772 regions worldwide are presented elsewhere; The Climate change Initiative Coastal Sea Level  
773 Team, 2020). Although the coastal trends within the 2-3 km to the coast are slightly lower than  
774 those reported above, exactly the same behavior is found, as shown in Fig.20 that compares  
775 coastal trends over 2002-2016 and 2002-2018. Thus, the trend increase close to the coast  
776 observed at Senetosa is not due to the limited length of the time series, although its amplitude  
777 decreases as the record length increases. Similarly, the geophysical correction trends present the  
778 same behavior over both time spans. It is worth mentioning that in the extended study (2002-  
779 2018), among the 429 studied coastal sites, coastal trends do not in general differ from open  
780 ocean trends (within  $\pm 1$  mm/yr), except at a few sites (The Climate Change Initiative Coastal  
781 Sea Level Team, 2020), Senetosa is one of them. This is why we made a focus on that particular  
782 site.

783

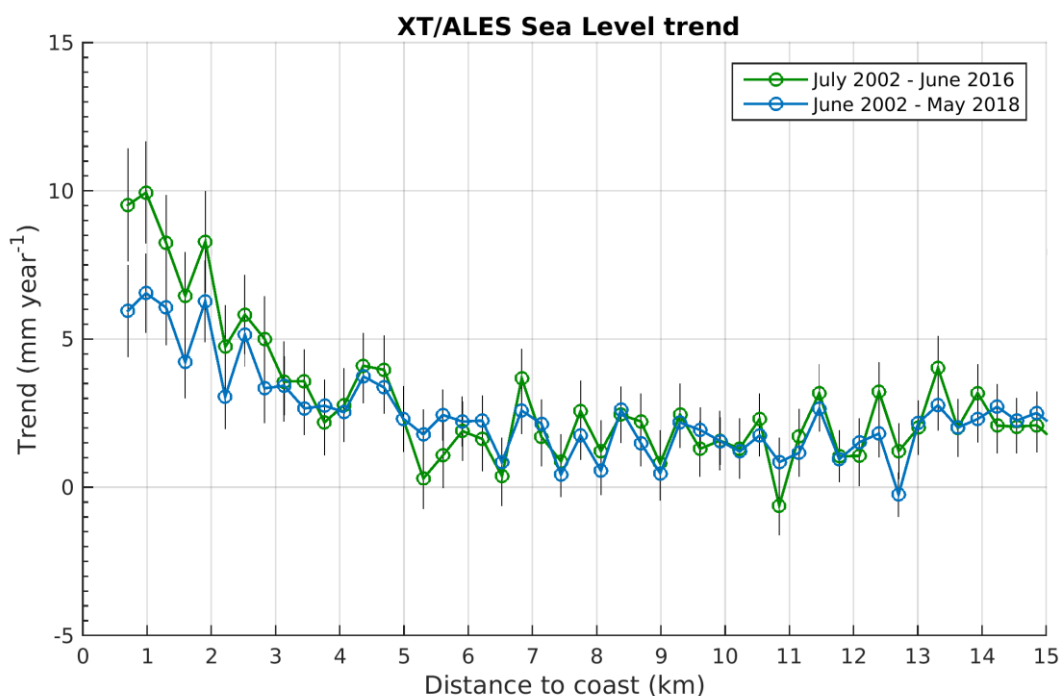
784

785



786

787



788 *Fig.20. Altimetry-based sea level trends at Senetosa, over two periods: (1) July 2002-June*  
 789 *2016, green curve and (2) June 2002-May 2018, blue curve. Black vertical bars*  
 790 *correspond to trend uncertainties.*

791

792 Among the physical mechanisms able to explain the coastal trend increase in the study region,  
 793 we have first explored waves, then currents. We investigated the wave effect on sea level  
 794 along the Jason track and found that wave set up has a too small magnitude and is localized  
 795 too close to the shore to explain the observed continuous SLA trend increase in the last 4-5  
 796 km to the coast. On the other hand, the correlation reported between altimetry-based SLAs  
 797 and SWH very likely results from the imperfect ssb correction applied to the data.  
 798 Nevertheless, if less accurate in the coast vicinity, the ssb trend seems unable to explain the  
 799 reported SLA trend increase. We next investigated the effect of coastal currents. Using the  
 800 MARS3D high resolution model developed by IFREMER for coastal studies, we noted the  
 801 presence of a winter current along the Senetosa coastline. Projection of this current along the  
 802 Jason track (for January 2014) shows a step increase in intensity over exactly the same  
 803 distance to the coast as the SLA trend increase. This may be an indication of a current-related  
 804 origin. More studies are definitely needed to confirm the results presented here. However, if  
 805 further investigations confirm the effect of currents, it will be a demonstration that small-  
 806 scale processes acting in the vicinity of the coast may have the capability to make coastal sea  
 807 level changes drastically different from what we measure offshore with classical altimetry.

808

809

810

**811 Acknowledgements**

812  
813 This study is a contribution to the ESA Climate Change Initiative (CCI+) Sea Level project.  
814 Yvan Gouzenes is supported by an engineer grant in the context of this project (ESA SL\_cci+  
815 contract number 4000126561/19/I-NB). We thank a number of colleagues for very fruitful  
816 discussions on the effect of waves on tide gauges and coastal sea level, in particular (by  
817 alphabetic order) Angel Amores, Xavier Bertin, Svetlana Jevrejeva, Goneri Le Cozannet,  
818 Marta Marcos, Judy Wolf and Phil Woodworth. We also thank two anonymous reviewers and  
819 the Editor for their comments and suggestions to improve the manuscript.

820

821

**822 Data availability**

823 The coastal sea level data analyzed in this study are available from the Nature Scientific Data  
824 article (The Climate change Initiative Coastal Sea Level Team, 2020). The ERA wave field  
825 data from the ERA5 reanalysis are available from the following web site:  
826 <https://www.ecmwf.int/en/forecasts/datasets/reanalysis-datasets/era5>.  
827 [The MARS3D model can be downloaded from the web site:](http://www.ifremer.fr/docmars/html/doc.basic.intro.html)  
828 <http://www.ifremer.fr/docmars/html/doc.basic.intro.html>)

829  
830  
831  
832  
833  
834  
835  
836  
837  
838  
839  
840  
841  
842  
843  
844  
845  
846  
847  
848  
849  
850  
851  
852  
853  
854  
855  
856  
857  
858  
859  
860  
861  
862  
863  
864  
865  
866  
867  
868  
869  
870  
871  
872  
873  
874  
875  
876  
877  
878  
879  
880  
881  
882

## References

- Ablain M., Legeais J.F., Prandi P., et al., 2017. Altimetry-based sea level, global and regional scales, *Surveys in Geophysics*, 38, 7-31, <https://doi.org/10.1007/s10712-016-9389-8>.
- Almar, R., E. Kestenare, J. Reyns, J. et al., 2015. Response of the Bight of Benin (Gulf of Guinea, West Africa) coastline to anthropogenic and natural forcing, Part1: Wave climate variability and impacts on the longshore sediment transport, *Continental Shelf Research*, 110, 48-59, <https://doi.org/10.1016/j.csr.2015.09.020>.
- Birol F. and C. Delebecque, 2014. Using high sampling rate (10/20 Hz) altimeter data for the observation of coastal surface currents: A case study over the northwestern Mediterranean Sea, *J. Mar. Syst.*, <https://doi.org/10.1016/j.jmarsys.2013.07.009>.
- Birol F., N.X Fuller, F. Lyard, et al., 2017. Coastal applications from nadir altimetry: example of the X-TRACK regional products. *Advances in Space Research*, 59, 936-953, <https://doi.org/10.1016/j.asr.2016.11.005>.
- Bruschi A., Buffoni G., Elliott A.J., Manzella G., 1981. A numerical investigation of the wind-driven circulation in the Archipelago of La Maddalena, *Oceanol. Acta*, 4, 3, 289-295.
- Bonnefond, P., Exertier, P., Laurain, O., Ménard, Y., Orsoni, A., Jan, G., Jeansou, E., 2003a, Absolute calibration of Jason-1 and TOPEX/Poseidon altimeters in Corsica, in: Special Issue on Jason-1 Calibration/ Validation, Part 1. *Mar. Geod.* 26(3-4), pp. 261-284, <https://doi.org/10.1080/714044521>.
- Bonnefond, P., Exertier, P., Laurain, O., Ménard, Y., Orsoni, A., Jeansou, E., Haines, B.J., Kubitschek, D.G., Born, G.H. Leveling sea surface using a GPS catamaran, 2003b, in: Special Issue on Jason-1 Calibration/ Validation, Part 1. *Mar. Geod.* 26(3-4), 319-334, <https://doi.org/10.1080/714044524>.
- Bonnefond, P., Exertier, P., Laurain, O., Jan, G., 2010, Absolute calibration of Jason-1 and Jason-2 altimeters in Corsica during the formation flight phase, in: Special Issue on Jason-2 Calibration/Validation, Part 1. *Mar. Geod.* 33(S1), 80-90, <https://doi.org/10.1080/01490419.2010>.
- Bonnefond, P., B. Haines and C. Watson. In Situ Calibration and Validation: A Link from Coastal to Open-ocean altimetry, 2011, in Coastal Altimetry, chapter 11, pp 259-296, edited by S. Vignudelli, A. Kostianoy, P. Cipollini, J. Benveniste, Springer, ISBN: 978-3-642-12795-3. [https://doi.org/10.1007/978-3-642-12796-0\\_11](https://doi.org/10.1007/978-3-642-12796-0_11)
- Bonnefond, P., Exertier, P., Laurain, O., Guinle, ., F m nias, ., 201 , Corsica: A 20-Yr Multi-Mission Absolute Altimeter Calibration Site, *Advances in Space Research*, Special Issue « 25 Years of Progress in Radar Altimetry », <https://doi.org/10.1016/j.asr.2019.09.049>.
- Carrere, L. and Lyard, F. 2003. Modeling the barotropic response of the global ocean to atmospheric wind and pressure forcing- comparisons with observations. *J. Geophys. Res.* 30 (6), 1275. <http://dx.doi.org/10.1029/2002GL016473>.
- Carrere L., Lyard, F., Cancet, M., Guillot, A., Roblou, L., 2012. FES2012: A new global tidal model taking taking advantage of nearly 20 years of altimetry, Proceedings of meeting "20 Years of Altimetry", Venice 2012.

- 883 Cartwright, D. E. and R. J. Taylor, 1971. New computations of the tide-generating potential,  
884 *Geophys. J. R. Astron. Soc.*, 23, 45-74.  
885
- 886 Cartwright, D. E. and Edden, A. C., 1973. Corrected Tables of Tidal Harmonics. *Geophysical Journal*  
887 *of the Royal Astronomical Society*, 33: 253-264. doi:10.1111/j.1365-246X.1973.tb03420.x.  
888
- 889 Church, J. A. et al., 2013: Sea Level Change. In: Climate Change 2013: The Physical Science  
890 Basis. Contribution of Working Group I to the Fifth Assessment Report of the  
891 Intergovernmental Panel on Climate Change [Stocker, T. F., D. Qin, G. K. Plattner, M.  
892 Tignor, S. K. Allen, J. Boschung, A. Nauels, Y. Xia, V. Bex and P. M. Midgley (eds.)].

- 893 Cambridge University Press, Cambridge, United Kingdom and New York, NY, USA, 1137-  
894 1216.
- 895 Cipollini P., J. Benveniste, F. Birol, et al., 2018. Satellite altimetry in coastal regions. In  
896 'Satellite altimetry over the oceans and land surfaces', Stammer & Cazenave Edts, CRC  
897 Press, Taylor and Francis Group, Boca Raton, London, New York, pp 343-373,  
898 <https://doi.org/10.1201/9781315151779-11>  
899
- 900 Climate Change Initiative Coastal Sea level Team (The), 2020, A database of coastal sea level  
901 anomalies and associated trends from satellite altimetry from 2002 to 2018, in revision, *Nature*  
902 *Scientific Data*.  
903
- 904 Cucco A et al., 2012, A high-resolution real-time forecasting system for predicting the fate of  
905 oil spills in the Strait of Bonifacio (western Mediterranean Sea), *Marine Pollution Bulletin*,  
906 64, 1186-1200, doi:10.1016/j.marpolbul.2012.03.019.  
907
- 908 Dieng, H., A. Cazenave, B. Meyssignac and M. Ablain, 2017: New estimate of the current  
909 rate of sea level rise from a sea level budget approach. *Geophysical Research Letters*, 44 (8),  
910 3744-3751, <https://doi.org/10.1002/2017GL073308>.  
911
- 912 Dodet G., Melet A., Ardhuin F., Bertin X., Idier D. and Almar R., 2019. The contribution of  
913 wind-generated waves to coastal sea level changes, *Surveys in Geophysics*, 40, 1563-1601,  
914 <https://doi.org/10.1007/s10712-019-09557-5>.  
915
- 916 Durand F., Piecuch C., Cirano M. et al., 2019. Impact of continental freshwater runoff on  
917 coastal sea level, *Surveys in Geophysics*, 40:1437–1466, [https://doi.org/10.1007/s10712-019-](https://doi.org/10.1007/s10712-019-09536-w)  
918 09536-w.  
919
- 920 Fernandes, M.J., Lazaro, C., Ablain, M., Pires, N., 2015. Improved wet path delays for all ESA  
921 and reference altimetric missions. *Remote Sens. Environ.* 169, 50–74,  
922 <http://dx.doi.org/10.1016/j.rse.2015.07.023>.
- 923 Gerigny O., Coudray S., Lapucci C., Tomasino C., Bisgambiglia P.A., Galgani F., 2015,  
924 Small-scale variability of the current in the Strait of Bonifacio, *Ocean Dynamics*, 65, 8, 1165-  
925 1182, <http://dx.doi.org/10.1007/s10236-015-0863-5>.  
926
- 927 Jebri, F., Birol, F., Zakardjian, B., Bouffard, J., Sammari, C., 2016. Exploiting coastal altimetry  
928 to improve the surface circulation scheme over the Central Mediterranean Sea: circulation In  
929 The Central Mediterranean. *J. Geophys. Res. Oceans* 121 (7), 4888–4909. [http://](http://dx.doi.org/10.1002/2016JC011961)  
930 [dx.doi.org/10.1002/2016JC011961](http://dx.doi.org/10.1002/2016JC011961).  
931
- 932 Lazure P and Dumas F, 2008, An external–internal mode coupling for a 3D hydrodynamical  
933 model for applications at regional scale (MARS), *Advances in Water Resources*, 31:233-250,  
934 doi:10.1016/j.advwatres.2007.06.010.  
935
- 936 Legeais J.F., Ablain M., Zawadzki L. et al., 2018. An improved and homogeneous altimeter  
937 sea level record from the ESA Climate Change Initiative, *Earth Syst. Sci. Data*, 10, 281-301,  
938 <https://doi.org/10.5194/essd-10-281-2018>.  
939
- 940 Léger F., F. Birol, F. Niño, M. Passaro, F. Marti and A. Cazenave, 2019, "X-Track/Ales  
941 Regional Altimeter Product for Coastal Application: Toward a New Multi-Mission Altimetry  
942 Product at High Resolution," IGARSS 2019 - 2019 IEEE International Geoscience and Remote  
943 Sensing Symposium, Yokohama, Japan, 8271-8274,  
944 <https://doi.org/10.1109/IGARSS.2019.8900422>.

- 945  
946 Manzella G.M.R., 1985, Fluxes across the Corsica Channel and coastal circulation in the East  
947 Ligurian Sea, North-Western Mediterranean, *Oceanol. Acta*, 8, 1, 29-35.  
948  
949 Marti F., Cazenave A., Birol F., Passaro, M. Leger F., Nino F., Almar R., Benveniste J. and  
950 Legeais J.F., 2019, Altimetry-based sea level trends along the coasts of western Africa, *Adv.*  
951 *in Space Res.*, published online 24 May2019, <https://doi.org/10.1016/j.asr.2019.05.033>,.

- 952
- 953 Melet, A., Almar, R. and Meyssignac, B., 2016. What dominates sea level at the coast: a  
 954 case study for the Gulf of Guinea. *Ocean Dyn.* 66, 623–636,  
 955 <https://doi.org/10.1007/s10236-016-0942-2>.
- 956 Melet A., Meyssignac B. Almar R. et al., 2018. Under-estimated wave contribution to  
 957 coastal sea-level rise, *Nature Climate Change*, 8, 234–239, [https://doi.org/10.1007/s10236-](https://doi.org/10.1007/s10236-016-0942-2)  
 958 [016-0942-2](https://doi.org/10.1007/s10236-016-0942-2).
- 959 Nerem, R. S. et al., 2018: Climate-change–driven accelerated sea-level rise detected in the  
 960 altimeter era. *Proceedings of the National Academy of Sciences*,  
 961 <https://doi.org/10.1073/pnas.1717312115>.  
 962
- 963 Passaro M., Cipollini P., Vignudelli S. et al., 2014. ALES: A multi-mission subwaveform  
 964 retracker for coastal and open ocean altimetry. *Remote Sensing of Environment* 145, 173–189,  
 965 <https://doi.org/10.1016/j.rse.2014.02.008>.
- 966 Passaro M., Cipollini P., Benveniste J., 2015, Annual sea level variability of the coastal  
 967 ocean: the Baltic Sea-North Sea transition zone. *J Geophys Res Oceans* 120(4):3061–3078,  
 968 <https://doi.org/10.1002/2014JC010510>.
- 969 Passaro M., Zulfikar Adlan N. and Quartly G.D., 2018. Improving the precision of sea level  
 970 data from satellite altimetry with high-frequency and regional sea state bias corrections.  
 971 *Remote Sensing of Environment*, 245–254, <https://doi.org/10.1016/j.rse.2018.09.007>.
- 972 Piecuch C.G., Bittermann K., Kemp A.C. et al., (2018). River-discharge effects on United  
 973 States Atlantic and Gulf coast sea-level changes, *PNAS*, vol. 115, no. 30, 7729–7734,  
 974 <https://doi.org/10.1073/pnas.1805428115>.
- 975
- 976 Sciascia R., Magaldi M. and Vetrano A., 2019, Current reversal and associated variability  
 977 within the Corsica Channel: The 2004 case study, *Deep-Sea Research Part I*, 144, 39–51.  
 978
- 979 SROCC 2019: IPCC Special Report on the Ocean and Cryosphere in a Changing Climate  
 980 [H.-O. Pörtner, D.C. Roberts, V. Masson-Delmotte, P. Zhai, M. Tignor, E. Poloczanska, K.  
 981 Mintenbeck, A. Alegría, M. Nicolai, A. Okem, J. Petzold, B. Rama, N.M. Weyer (eds.)].et al.].  
 982 In press.
- 983 Stammer D, Cazenave A, Ponte RM, Tamisiea ME (2013) Causes for contemporary regional  
 984 sea level changes. *Annu Rev Mar Sci.* <http://doi.org/10.1146/annurev-marine-121211-172406>  
 985
- 986
- 987 Wahr, J.M., 1985. Deformation Induced by Polar Motion. *J. Geophys. Res.*, 90 (B11), 9363–  
 988 9368.
- 989
- 990 Vignudelli S. , A. G. Kostianoy, P. Cipollini, and J. Benveniste (Eds.), 2011, Coastal  
 991 Altimetry, Springer, Berlin, <https://doi.org/10.1007/978-3-642-12796-0>.
- 992 The WCRP Global Sea Level Budget Group (2018). Global sea level budget, 1993-present.  
 993 *Earth Syst. Sci. Data*, 10, 1551–1590, <http://doi.org/10.5194/essd-10-1551-2018>.
- 994 Woodworth P., Melet A., Marcos M. et al., 2019. Forcing Factors Causing Sea Level Changes  
 995 at the Coast, *Surveys in Geophysics*, <https://doi.org/10.1007/s10712-019-09531-1>.

996  
997 Wöppelmann, G., and M. Marcos (2016), Vertical land motion as a key to understanding sea  
998 level change and variability, *Rev. Geophys.*, 54, 64–92,  
999 <https://doi.org/10.1002/2015RG000502>.

1000

1001



**RESPONSES TO THE EDITOR'S COMMENTS (*in italics*)**

1002  
1003  
1004 **Topic Editor Decision: Publish subject to minor revisions (review by editor)** (31 Jul 2020) by [Joanne](#)  
1005 [Williams](#)  
1006 Comments to the Author:  
1007 Dear authors,  
1008  
1009 Thank-you for your revised manuscript, and response to the reviews. There are a few minor issues  
1010 remaining, as follows.  
1011  
1012 Table 1: please be consistent in usage of Ku-band (ideally \$K\_u\$)  
1013  
1014 *Corrected*  
1015  
1016 Table 1: sea-state bias (spelling)  
1017  
1018 *Corrected*  
1019  
1020 line 159: western Mediterranean Sea  
1021  
1022 *Corrected*  
1023  
1024 line 167: "Senetosa is operating"? The place can't operate it. Perhaps "Since 1998 a calibration site has  
1025 operated near the Senetosa lighthouse, with support from..."?  
1026  
1027 *Modified as suggested*  
1028  
1029 line 176: You could tidy this a little, eg "M4/M5 as a few cm apart, sheltered from the northwest-ward  
1030 wind, whilst M3 is a 1.7km eastward, more exposed to open-sea conditions. "  
1031  
1032 *Modified as suggested*  
1033  
1034 Fig 1: Ensure the copyright is correctly handled for the Google earth image - See [https://www.ocean-](https://www.ocean-science.net/for_authors/manuscript_preparation.html)  
1035 [science.net/for\\_authors/manuscript\\_preparation.html](https://www.ocean-science.net/for_authors/manuscript_preparation.html)  
1036  
1037 [OK](#)  
1038  
1039 line 210: Outliers are omitted in computing the regression line.  
1040  
1041 *Corrected*  
1042  
1043 line 245, 250 (and check elsewhere): "Figure 4 shows..." or "as shown in Fig. 4"  
1044  
1045 *Corrected*  
1046  
1047 line 255: Grammar. I suggest: "In coastal areas, precision of sea surface height from altimetry is limited  
1048 by inaccuracies in some of the applied geophysical corrections (including sea state bias, wet  
1049 tropospheric correction, dynamical atmospheric correction and ocean tides) and from the distorted  
1050 shape of the radar waveforms as the satellite approaches land (Vignudelli et al., 2011 and Cipollini et al.,  
1051 2018).  
1052  
1053 *Modified as suggested*  
1054  
1055 line 260: Bit vague. I think you mean that data that is not flagged can still have errors due to coastal  
1056 proximity?  
1057  
1058 *Modified*

1059  
 1060 line 265/269 : Try not to switch tense. examined?  
 1061  
 1062 *Modified*  
 1063  
 1064 line 269: reads like  $d(ssb)/d(\text{distance to coast})$ . I suggest "We plotted trends in geophysical correction  
 1065 against distance to the coast, for sea-state bias..."  
 1066  
 1067 *Modified as suggested*  
 1068  
 1069  
 1070 Fig 6b is unnecessary. Suggest line 329 becomes "We resampled the along-track sea-level records  
 1071 keeping only the 80% of data common to all along track positions at a given time."  
 1072  
 1073 *Fig.6b has been deleted*  
 1074 *Line 329 modified as suggested*  
 1075  
 1076 line 333 cut "then"  
 1077  
 1078 *Done*  
 1079  
 1080 Fig 7: as a general rule for color-vision accessibility, avoid red vs green lines. Replot if possible, however  
 1081 it does not significantly affect the message of this figure so I don't insist on it. However in Fig 20 it does  
 1082 matter, please replot.  
 1083  
 1084 *We have not modified the figures except Fig.20 which has been redrawn (blue instead of red)*  
 1085  
 1086 line 383: full stop.  
 1087  
 1088 *Done*  
 1089  
 1090 line 515: cut "well"  
 1091  
 1092 *Done*  
 1093  
 1094 Fig 10: would be more intuitive rotated to align with the map. However it is not essential.  
 1095  
 1096 *In effect, this is not essential*  
 1097  
 1098 Fig 12: It would have been good to see the altimetry results alongside here.  
 1099  
 1100 *It will be the purpose of another paper in preparation where we compare tide gauge records with*  
 1101 *coastal SLA time series at Senetosa and several other sites*  
 1102  
 1103 line 595: "it is very unlikely that wave set up explains the reported coastal sea level trend."  
 1104  
 1105 *Modified as suggested*  
 1106  
 1107 lines 604-715: The argument in this section is rambling and hard to follow. It needs tidying up and  
 1108 probably condensing. You can simplify a lot of sentences.  
 1109  
 1110 As I understand your argument ...  
 1111 Could waves explain the SLA trends approaching the coast? SWH at a nearby ERA grid point has little  
 1112 correlation with SLA at 15km, but has some correlation with SLA at the coast, Fig15 & Fig 16a. One  
 1113 mechanism for waves to affect the altimetry corrections is via ssb. SWH at the ERA grid point does not  
 1114 correlate well with ssb near the coast (Fig 16b & Fig 17). So it is possible the wrong ssb is used as an  
 1115 altimetry correction near the coast (slightly better in ALES). Therefore though the waves do correlate

1116 with SLA, it's not via ssb, so it's not causal. So despite fig 16a, the argument in the first part of 6.1 still  
 1117 holds? You say you have eliminated waves as the explanation.

1118  
 1119 However in section 6.2 we learn that the winds are highly seasonal and affect the local currents.  
 1120 Seasonal changes in wind direction would directly affect the local SWH, since sometimes the coast will  
 1121 be sheltered. More localised wind and wave information would be very helpful here. Otherwise I think  
 1122 you can only say that there is no strong evidence for waves and ssb causing the trend in SLA.

1123  
 1124 If I've got this right it's after a lot of unpicking. Please clarify. If I've got it wrong, then this *\*really\** needs  
 1125 clarifying.

1126 *It seems that our text was unclear because the above comment is exactly the opposite of what we*  
 1127 *wanted to say, ie., that the correlation between waves and SLA is do to the wrong SSB.*  
 1128 *Schematically:*

1129 *1) SLA without SSB correction is always correlated with SWH (the SSB phenomenon is a*  
 1130 *function that is directly proportional to SWH. It is THERE until we remove it with a correction)*

1131 *2) If we apply the SSB correction correctly, we decrease the correlation between SLA and SWH*

1132 *3) If the SSB correction is wrong, the correlation remains. This is what we see very close to the*  
 1133 *coast.*

1134 *The confusion comes from the fact that, although we are focusing on the explanation that the ssb*  
 1135 *correction is not being effective very very close to the coast, we still (during the section) keep*  
 1136 *open the possible explanation that the correlation between SWH and SLA is physical ("This*  
 1137 *clearly suggests that computed SLAs are impacted by waves in the last few km to the coast on a*  
 1138 *broad range of time scales").*

1139 *We have modified the text of the revised version to make the argumentation clearer. We have also*  
 1140 *added a short introduction to explain what we want to demonstrate.*

1141  
 1142 specifics from this section:  
 1143 line 604: cut "However"

1144  
 1145 *Done*

1146  
 1147 line 609: we consider sea-level anomalies...

1148  
 1149 *Corrected*

1150  
 1151 line 610: cut "mesh"

1152  
 1153 *Done*

1154  
 1155 line 610: Please indicate the position of the ERA5 grid point you use on one of the maps. ERA5 grid  
 1156 spacing is about 30km so it matters. It is a pity you don't have anything finer resolution here.

1157  
 1158 *We have added a sentence in the text indicating the position of the closest grid mesh to Senetosa*  
 1159

1160 line 638-640: No. Fig 16a doesn't show the interannual correlation, because it is swamped by the  
 1161 seasonal signal. You'll have to replot this or at least recalculate R after filtering the seasonal out.

1162  
 1163 *The correlation is mostly based on the seasonal signal but as the amplitude of the latter varies with time*  
 1164 *in the same way in both time series, this indicates that the correlation also holds at interannual time*  
 1165 *scale*

1166  
1167 line 693: The correlations are really rather weak here. Suggest "As expected, ssb is correlated with wave  
1168 height away from the coast, but..." It is difficult to see any relationship from the figure. Replot with the  
1169 orange ssb curves on a different scale (eg use a right-hand axes).  
1170  
1171 *Modified as suggested*  
1172  
1173 line 699: You haven't calculated significance. Rephrase.  
1174  
1175 *Modified as suggested*  
1176  
1177 lines 729-733: could condense this.  
1178  
1179 *Done*  
1180  
1181 Fig 18 & 19: could be combined. And why zonal only? You need the meridional component too to give  
1182 the along-shore current.  
1183  
1184 *Only the zonal components shows some trend. More investigation is on going using the MARS3D model*  
1185 *around Senetosa and this will be the subject of another paper in preparation.*  
1186  
1187 Please indicate 15 km along-track distance on at least one map.  
1188  
1189 *Done in the text*  
1190  
1191 Although you can't derive a trend from the MARS3d model, and it's fair enough to pass on the coastal  
1192 oceanography to another study, it would be very helpful to do a seasonal comparison, perhaps plot a  
1193 different season in Fig 18.  
1194  
1195 *See above comment*  
1196  
1197 line 832: cut "elongated"  
1198  
1199 *Done*  
1200  
1201 line 834: an indication  
1202  
1203 *Corrected*  
1204  
1205 You have not met all requirements in  
1206 [https://www.ocean-science.net/for\\_authors/manuscript\\_preparation.html](https://www.ocean-science.net/for_authors/manuscript_preparation.html)  
1207 Please attend particularly to data referencing, but check through other requirements as well. Don't rely  
1208 on the typesetter to find them!  
1209 The MARS3d model, ERA5 data (they have a standard format statement required), altimetry data all  
1210 need correct acknowledgement and statement of where to access the data. This should be in a Data  
1211 Availability section.  
1212  
1213 *A Data availability section added*